AD-A064 213 AIR FORCE INST OF TECH WRIGHT-PATTERSON AFB OHIO SCH--ETC F/G 20/5
ANALYTIC ELECTRON ENERGY DISTRIBUTION FUNCTIONS FOR ELECTRIC DI--ETC(U)
DEC 78 T E GIST

UNCLASSIFIED AFIT/GEP/PH/78D-4 NL

1 OF 2
AD A064213

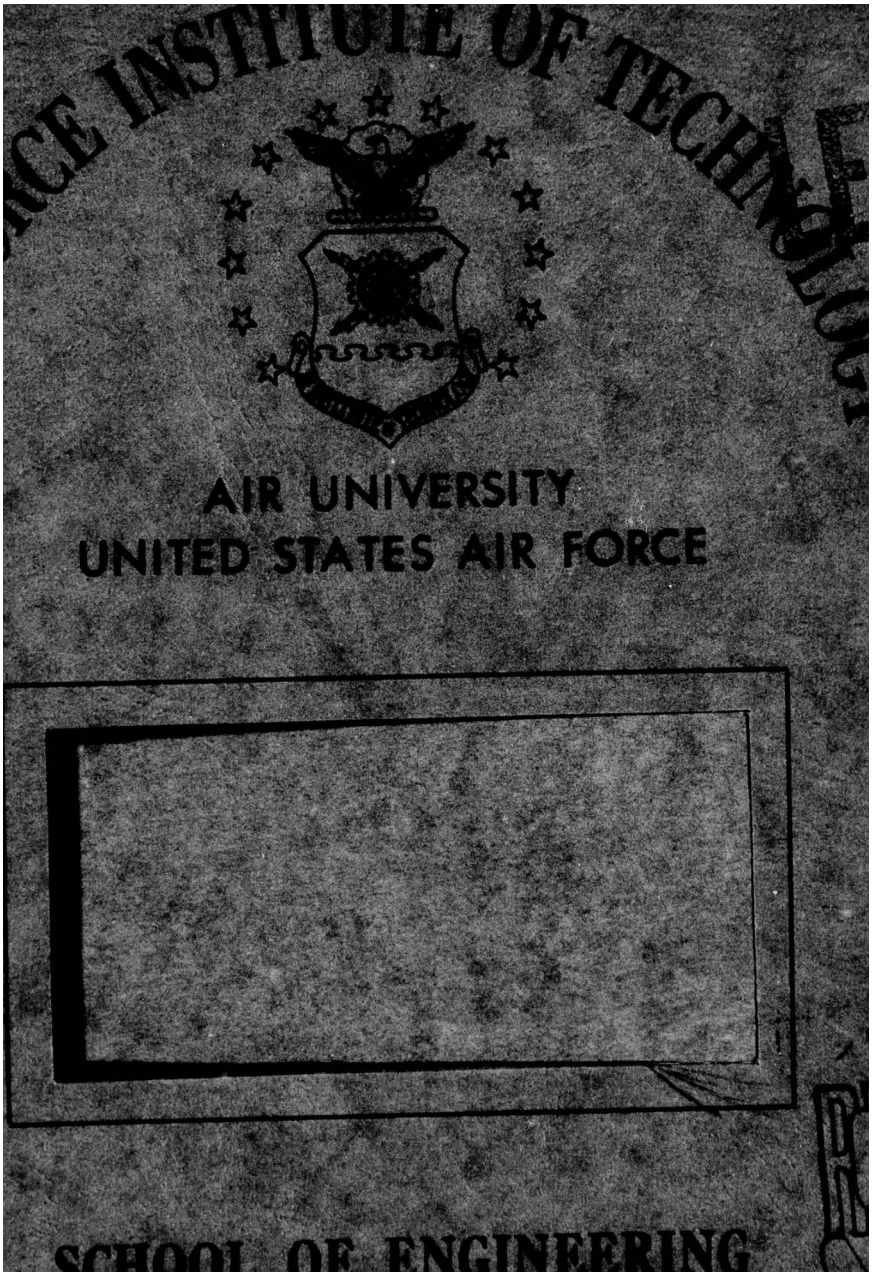
ACE INSTITUTE OF TECHNOLOGY
AIR UNIVERSITY
UNITED STATES AIR FORCE
SCHOOL OF ENGINEERING

AFIT/GEP/PH/78D-4

(1)

LEVEL II

ANALYTIC ELECTRON ENERGY DISTRIBUTION FUNCTIONS FOR ELECTRIC DISCHARGE LASERS

THESIS

AFIT/GEP/PH/78D-4 Thomas E. Gist
Capt USAF

Approved for public release; distribution unlimited

(14) AFIT/GEP/PH/78D-4

(6) ANALYTIC ELECTRON ENERGY DISTRIBUTION FUNCTIONS FOR ELECTRIC DISCHARGE LASERS.

~~THESIS~~

(9) Master's thesis,

Presented to the Faculty of the School of Engineering

of the Air Force Institute of Technology

Air University

in Partial Fulfillment of the

Requirements for the Degree of

Master of Science

by

(10) Thomas E. Gist, B.S.

Capt USAF

Graduate Engineering Physics

(11) December 1978 (12) 100 p.

Approved for public release; distribution unlimited.

Acknowledgemnts

I would like to acknowledge the guidance and assistance of Philip Nielsen, who provided the impetus for this thesis, and without whose help, completion would have been very difficult. I would also like to acknowledge the advice and assistance of Allen Hunter, who on several occasions provided the insight necessary to get past difficulties. I would like to acknowledge the aid and support of William Ercoline, Harold Hastings, and Edward Seward. On many occasions they were able to provide information they had discovered that saved me much time and effort. Finally, I must acknowledge the support, aid and understanding of my wife, Karen. Her long hours of typing and plotting were instrumental in the completion of this thesis; her understanding support was vital.

Thomas E. Gist

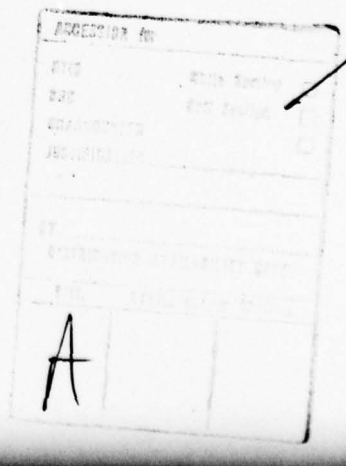

Contents

List of Figures

List of Tables

Abstract

The Boltzmann equation for electrons is solved for background gases of one or two excited levels under conditions typical of electric discharge lasers. Reaction rates are assumed constant above a threshold energy, and the electron heating rate is assumed independent of electron energy. Elastic and superelastic collisions were not considered. Numerical solutions from a program developed in conjunction with Seward, Hastings, and Ercoline are in excellent agreement with the analytic solutions. The analytic solutions are compared to numerical solutions that use realistic cross sections; the analytic solutions agree well for some cross sections. It is possible to determine *a priori* which realistic cases the analytic model will fit. For these cases it is possible to estimate pumping rates for upper levels with reasonable success. In some cases it is possible to model systems with more than two excited levels. Limitations to the analytic model and validity of the assumptions are discussed. Programs for evaluating the analytic solutions on a Texas Instruments programmable 59 calculator are included.

ANALYTIC ELECTRON ENERGY DISTRIBUTION FUNCTIONS FOR ELECTRIC DISCHARGE LASERS

I Introduction

Background

There is a considerable interest in the United States Air Force in developing high energy lasers. One of the problems that must be solved in this development process is predicting the electron energy distribution function produced by some heating machanism in the plasma in a laser gain tube. To date this has been attempted both numerically and analytically, without complete success.

The numerical methods will produce a value for the number of electrons with energies between ϵ and $\epsilon + d\epsilon$ at a given time, for a given set of initial conditions. But it is then impossible to determine from this solution the same information for a different set of initial conditions. In addition, without having a second independent solution to the problem for at least some cases that can be compared to the numerical solution, it is difficult to be certain that the numerical results are valid.

The existing analytic solutions also lack completeness for several reasons. It is not always possible to obtain analytic solutions. Those solutions that do exist are based on versions of the Boltzmann equation that have been simpli-

fied by various assumptions; although these assumptions make solving the equation simpler, they also reduce the accuracy of the solutions. In addition, these assumptions make the solutions valid only for particular classes of initial conditions.

The analytic models are very important, however. Although they are not valid for all physical situations due to the various assumptions involved, there will be physical situations of interest that the analytic solutions will model accurately. In these cases, the analytic solutions can be used to verify the validity of the numerical solutions. In addition, the analytic models can indicate how the numerical solutions change as the physical situation changes. The analytic solutions can also give very important insight into the physical phenomena involved.

Problem Statement

Analytic solutions of the Boltzmann equation are developed which describe the electron distribution function in a plasma. The solutions developed eliminate some of the problems associated with previous analytic solutions and are compared to a series of numerical solutions of both idealized and realistic systems.

Definitions

Several definitions are needed for this discussion. The first of these is the electron distribution function $f(\epsilon)$. If $F(\epsilon)d\epsilon/N$ is the fraction of electrons with energies be-

tween ϵ and $\epsilon + d\epsilon$, then $f(\epsilon) = \frac{F(\epsilon)}{\epsilon^{\frac{1}{2}}}$. This form of the distribution function is chosen to simplify some of the output for the numerical solutions. The normalization factor N simplifies the derivation and is defined so that

$$\int_0^\infty \frac{f(\epsilon)\epsilon^{\frac{1}{2}}}{N}\, d\epsilon = \int_0^\infty \frac{F(\epsilon)}{N}\, d\epsilon = 1 \qquad (1\text{-}1)$$

The appropriate Boltzmann equation for $F(\epsilon)$ is

$$\frac{\partial F(\epsilon,t)}{\partial t} + \frac{\partial}{\partial \epsilon}\left[\frac{2}{3}\,\dot{\epsilon}\left(\frac{F(\epsilon,t)}{2} - \epsilon\,\frac{\partial F(\epsilon,t)}{\partial \epsilon}\right)\right] =$$

$$\sum_\beta \left[n_{\beta^*} F(\epsilon',t)\bar{R}_\beta(\epsilon') - n_\beta F(\epsilon,t) R_\beta(\epsilon)\right] \qquad (1\text{-}2)$$

where

$\dot{\epsilon}$ = rate of energy increase per electron per unit time(electron heating rate)

n_β = number density of species

n_{β^*} = number density of species β^* which is "inverse" to β

$R_\beta(\epsilon)$ = rate constant for the reaction $e(\epsilon) + \beta \longrightarrow e(\epsilon') + \beta^*$

$\bar{R}_\beta(\epsilon')$ = rate constant for the reaction $e(\epsilon') + \beta^* \longrightarrow e(\epsilon) + \beta$

β and β^* are the initial and final states of some transition.

$e(\epsilon)$ is an electron of energy ϵ (Ref 13: 2348-2349)

Another term that needs defining is "steady-state." For the purposes of this discussion, a steady state solution for the distribution function is one for which the distribution

function is a function of energy only, not time, over time scales of interest. Note that this does not require a constant electron density, but only that the proportion of electrons in any given energy range is constant.

Assumptions

Several assumptions are used in this thesis. First, it is assumed that a steady state condition exists after some initial transient phase; this phase typically lasts for a time on the order of picoseconds. Second, it is assumed that the electron density is low enough ($< 10^{10}$ cm^{-3}) that electron-electron interactions can be ignored. These two assumptions are direct consequences of the limitations in scope to be discussed later. Third, it is assumed that $f(\epsilon)$ is of the form

$$f(\epsilon) = c\left(\exp\left[-\frac{\epsilon}{kT(\epsilon)}\right]\right) \quad , \epsilon > X_\beta \tag{1-3}$$

where c is an arbitrary constant and k is Boltzmann's constant. Note that this differs from the normal Maxwellian distribution in that instead of T being a parameter characteristic of the distribution as a whole, it is a function of the electron energy ϵ. It is further assumed that

$$\epsilon >> kT(\epsilon) \quad , \epsilon > X_\beta \tag{1-4}$$

$$\frac{\partial T}{\partial \epsilon} >> kT\frac{\partial^2 T}{\partial \epsilon^2} \quad , \epsilon > X_\beta \tag{1-5}$$

The last three assumptions (Eqs (1-3), (1-4), and (1-5)), are based on observations of published distribution functions, as discussed in Chapter II. Finally, it is assumed that

$$\frac{n_o}{n_x} >> 1 \qquad (1\text{-}6)$$

where n_o is the neutral particle density

n_x is the excited particle density

This assumption is required to enable super-elastic collisions to be ignored. For gases at atmospheric pressure, n_x can approach 10^{10} - 10^{16} cm^{-3} before this assumption becomes invalid. Although these values can be exceeded in electric discharge lasers in some circumstances, the assumption would still be valid until n_x exceeded those levels.

The validity of Eqs (1-4) through (1-6) is addressed in more detail in Appendix A.

Scope

This thesis examines the distribution of an electron gas in the presence of a background gas. It deals with the steady-state case only. It includes background gases with both single and multiple excited levels. Superelastic collisions will not be considered analytically except to determine the limits of validity of the solutions, and electron-electron collisions are excluded.

Summary of Current Knowledge

At present there are few published works that deal

exactly with this problem, although there are several that deal with closely related problems. For example, Rockwood did considerable work in developing a numerical method of solving the Boltzmann equation, but did not find any analytic distribution functions (Ref 13). Nielsen, Canavan, and Rockwood used a quantum-kinetic approach to investigate gas breakdown numerically (Refs 10; 11; and 14). Englehardt and Phelps used numerical techniques to solve the Boltzmann equation in order to find excitation cross-sections (Ref 4). Elliott and Greene used numerical techniques to study the time evolution of the Boltzmann equation (Ref 3). Nighan used numerical techniques to find distribution functions in various gases (Ref 12). Frost and Phelps were able to solve the Boltzmann equation analytically for rotational excitations, but only by assuming that the rotational levels were so close together as to form a continuum; this assumption is invalid for vibrational or excitational levels. For these levels Frost and Phelps used numerical techniques (Ref 5). Long, Bailey, and Garscadden explicitly consider a spatially non-homogenous problem by using a first-order Laguerre expansion of the Boltzmann equation. They then use the zero-order function, f_o, (which corresponds to f in this paper) to find f_1. However, since their ultimate goal was drift velocities, which they could find without knowing f_o explicitly, they did not find an analytic distribution function corresponding to f (Ref 7).

Nielsen has one unpublished paper which addresses this

specific problem. In it he uses the same assumptions as this thesis to find an analytic form for $f(\epsilon)$, suggests how the solution might be extended, and discusses the impact of his solution on numerical programs. However, this thesis shows there is a minor error in Nielsen's paper; furthermore, Nielsen's paper does not actually extend the solution to three or more levels, nor does it include any extensive comparisons with numerical solutions (Ref 9).

Approach

This thesis is an extension of Nielsen's unpublished paper (Ref 9). Using the same general method, a corrected two level model is developed. This model is then extended to three levels, where the spacing between the two excited levels is greater than the spacing between the ground level and the first excited level. An example of a real system with these characteristics would be one with a low-lying group of closely-spaced vibrational levels, which could be approximated by a single lower excited level, and then a higher electronic level. Then it is shown how the solution can be extended to more than three levels, with arbitrary spacing.

While the analytic research was being done, a numerical program was also being developed in conjunction with E. D. Seward, W. R. Ercoline, and H. L. Hastings (Ref 15). This program was used to find distribution functions for comparison to the analytic solutions, to investigate how to best fit the idealized analytic solutions to real phenomena, and

to help verify the limits of applicability of the analytic solutions.

II. Solution of the Time Independent Boltzmann Equation for Inelastic Collisions

Rationale for Approach

The published literature contains examples that indicate that $F(\epsilon)$ approximates, at high enough energy, a Maxwellian distribution $\sim \epsilon^{\frac{1}{2}} \exp\left[\frac{-\epsilon}{kT}\right]$ (see Fig 1) (Refs 3; and 12). If the fluctuations from an ideal Maxwellian are slowly varying functions of energy, it seems plausible to represent $F(\epsilon)$ by a near-Maxwellian $\sim \epsilon^{\frac{1}{2}} \exp \frac{-\epsilon}{kT(\epsilon)}$. Now T is no longer a true temperature characteristic of the distribution as a whole, but is a slowly varying function of ϵ. Hopefully this representation will result in a form of the Boltzmann equation that can be readily solved.

Derivation of the Equation for $T(\epsilon)$

Boltzmann Equation for $F(\epsilon)$. It is assumed that the electrons are in the presence of a background gas of identical massive particles (which may be atoms or molecules). The particles have one or more excited states; the particles are massive enough that elastic collisions may be ignored. The electron density is assumed to be low enough for electron-electron interactions to be ignored. It is also assumed that the environment (and, as a consequence, $F(\epsilon)$) is spatially homogeneous and isotropic in energy space. These assumptions are quite reasonable for a typical electric discharge laser. Ionization will not be considered.

Under these conditions equation (1-2) can be derived

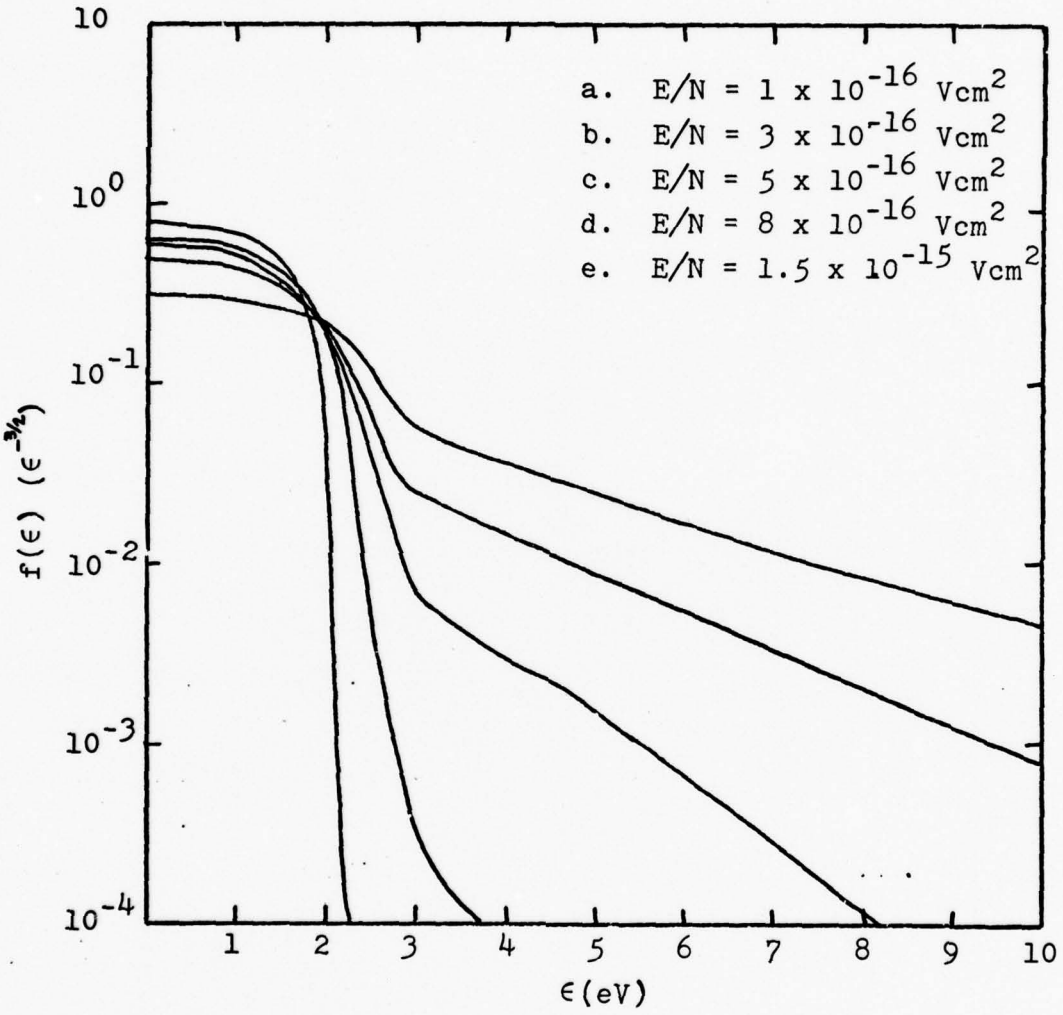

Figure 1. Published Distribution Functions in N_2 (Ref 12: 1992)

from Rockwood's formulation. The reverse reaction rate constants are related to the forward rates by the principle of micro-reversibility (Ref 2: 431).

Form for $\dot{\epsilon}$ and $R(\epsilon)$. It would be extremely difficult to solve equation (1-2) analytically using the experimentally derived rate constants and an electron-energy-dependent $\dot{\epsilon}$. Therefore, some simplifying assumptions will be made about $\dot{\epsilon}$ and the form of $R(\epsilon)$. First, $\dot{\epsilon}$ is assumed to be constant in energy space. Using an expression for $\dot{\epsilon}$ derived from Rockwood, it can be shown that this assumption is equivalent to assuming that the collision frequency of electrons with the background gas is independent of energy (Ref 13: 2348). Although this assumption only approximates the real cases, it does simplify the solution of the problem considerably.

Second, the following form for $R_\beta(\epsilon)$ is assumed:

$$R_\beta(\epsilon) = \begin{cases} 0, & \epsilon < X_\beta \\ R_\beta, & \epsilon \geq X_\beta \end{cases}$$

where X_β is the threshold energy for the excitation to the excited state β. Since R is proportional to $\sigma\epsilon^{\frac{1}{2}}$, where σ is the inelastic collision cross section, this assumption is equivalent to assuming that σ is proportional to $\epsilon^{-\frac{1}{2}}$ (see Fig 2). Again, this assumption only approximates real cross-sections. However, it simplifies the solutions considerably, and it appears from the numerical calculations discussed in Chapter III that the solutions are insensitive to the exact form of the cross-sections.

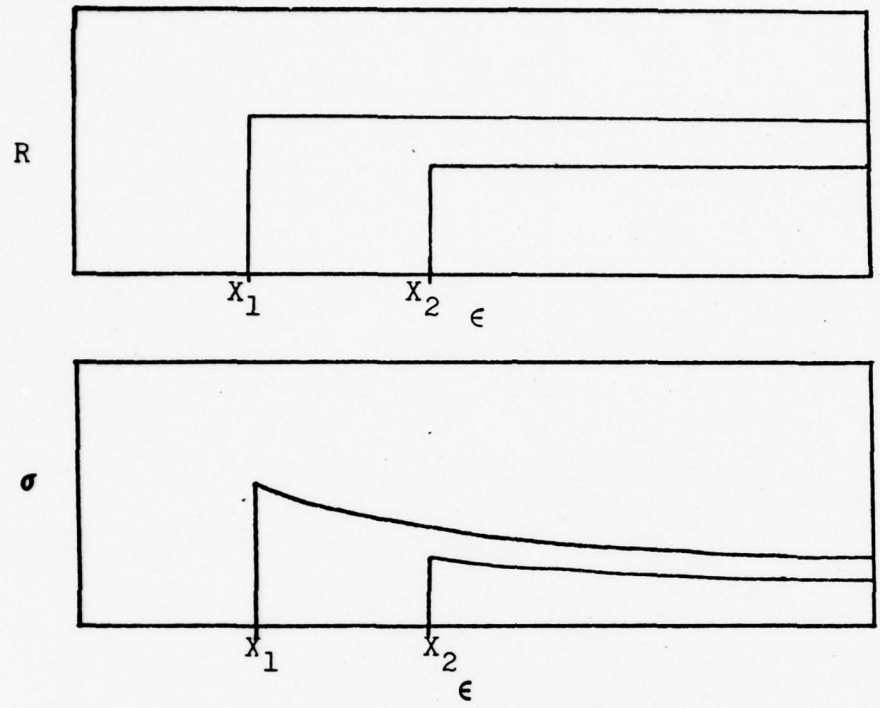

Figure 2. Analytic R and σ

Derivation of Equation for $T(\epsilon)$. For convenience in the derivation and in comparisons of analytic results to numerical results, a function $f(\epsilon)$ was defined such that $f(\epsilon) = \epsilon^{\frac{1}{2}} F(\epsilon)$. Consistent with the assumption that $F(\epsilon) \sim \epsilon^{\frac{1}{2}} \exp\left[\frac{-\epsilon}{kT(\epsilon)}\right]$ for high energies, an assumed form $f(\epsilon) = c\left(\exp\left[\frac{-\epsilon}{kT(\epsilon)}\right]\right)$ was used. Finally, from published numerical results, it was observed that $f(\epsilon)$ drops off over an energy range much less that ϵ, and does so fairly smoothly, for $\epsilon >> X$, as long as E/n_o is less than approximately 4×10^{-10} Vcm^2 (See Fig 1) (Refs 3; and 12). This led to two more assumptions, which are crucial to the derivation:

$$1)\ \frac{\epsilon}{kT} >> 1\ ,\ \text{for}\ \ \epsilon > X_\beta \qquad (\text{which implies}\ \ \frac{X_\beta}{kT} >> 1\ )$$

$$2)\ \frac{1}{kT}\frac{\partial T}{\partial \epsilon} >> \frac{\partial^2 T}{\partial \epsilon^2}\ ,\ \text{for}\ \ \epsilon > X_\beta\ . \qquad (2\text{-}2)$$

In Appendix A, it is shown that these assumptions are consistent with the solution found.

Using these definitions and assumptions, a straightforward but tedious derivation leads from Eq (1-2) to

$$0 = \frac{2\dot{\epsilon}\epsilon}{3(kT)^2} - \frac{4\dot{\epsilon}\epsilon^2}{3k^2T^3}\frac{\partial T}{\partial \epsilon} + \frac{2\dot{\epsilon}\epsilon^3}{3k^2T^4}\left(\frac{\partial T}{\partial \epsilon}\right)^2 + \sum_\beta \left[n_{\beta *} \exp\left(\frac{\epsilon}{kT(\epsilon)} - \frac{\epsilon'}{kT(\epsilon')} \right) \bar{R}_\beta(\epsilon') \left(\frac{\epsilon'}{\epsilon}\right)^{\frac{1}{2}} - n_\beta R_\beta(\epsilon) \right]\ ,\ \epsilon > X_\beta \qquad (2\text{-}3)$$

Solution for f(ϵ), Two-Level Case

ϵ > X. For the two-level case being considered, β can represent either the ground state or the excited state. Since ϵ' is the electron energy of the initial state of a reaction where the electron's final energy is ϵ,

$$\epsilon' = \begin{cases} \epsilon - X_\beta\ , & \text{for}\ \ \beta = \text{ground state} \\ \epsilon + X_\beta\ , & \text{for}\ \ \beta = \text{excited state} \end{cases} \qquad (2\text{-}4)$$

From the principle of micro-reversibility, it can be shown that $\bar{R}_\beta(\epsilon) = R_\beta(\epsilon + X_\beta)((\epsilon + X_\beta)/\epsilon)^{\frac{1}{2}}$ and $\bar{R}_\beta(\epsilon - X_\beta) = R_\beta(\epsilon)(\epsilon/(\epsilon - X_\beta))^{\frac{1}{2}}$ (Ref 2: 431). Using n_o for the ground state particle density, n_x for the excited state

particle density, and the assumed values for $R_\beta(\epsilon)$ results in

$$0 = \frac{2\dot{\epsilon}\epsilon}{3(kT)^2} - \frac{4\dot{\epsilon}\epsilon^2}{3k^2T^3}\frac{\partial T}{\partial \epsilon} + \frac{2\dot{\epsilon}\epsilon^3}{3k^2T^4}\left(\frac{\partial T}{\partial \epsilon}\right)^2 + n_x R(\epsilon)\exp\left(\frac{\epsilon}{kT(\epsilon)}\right.$$

$$\left. - \frac{(\epsilon - X)}{kT(\epsilon - X)}\right) - n_o R(\epsilon) + n_o R(\epsilon + X)\exp\left(\frac{\epsilon}{kT(\epsilon)}\right.$$

$$\left. - \frac{(\epsilon + X)}{kT(\epsilon + X)}\right)\left(\frac{\epsilon + X}{\epsilon}\right)^{\frac{1}{2}} - n_x R(\epsilon + X)\left(\frac{\epsilon + X}{\epsilon}\right)^{\frac{1}{2}} , \tag{2-5}$$

where the "β" subscripts have now been dropped and micro-reversibility has been used. Using the assumptions already made, and neglecting super-elastic collisions (which follows from the assumption that $n_x << n_o$), it is straightforward to show that, for $\epsilon > X$

$$0 = \frac{2\dot{\epsilon}\epsilon}{3(kT)^2} - \frac{4\dot{\epsilon}\epsilon^2}{3k^2T^3}\frac{\partial T}{\partial \epsilon} + \frac{2\dot{\epsilon}\epsilon^3}{3k^2T^4}\left(\frac{\partial T}{\partial \epsilon}\right)^2 - n_o R , \quad \epsilon > X \tag{2-6}$$

This equation has the general solution

$$T = \frac{1}{k}\left(\sqrt{\frac{\dot{\epsilon}}{6n_o R}}\right)\sqrt{\epsilon} + c' , \quad \epsilon > X \tag{2-7}$$

which leads to the general solution for $f(\epsilon)$ of

$$f(\epsilon) = c\exp\left(-\sqrt{\frac{6n_o R\epsilon}{\dot{\epsilon}}}\right) , \quad \epsilon > X \tag{2-8}$$

where c is a constant of integration, which will be evaluated later. For convenience, the constant factor in the exponen-

tial will be defined as follows:

$$\sqrt{\frac{6n_o R}{\dot{\epsilon}}} = \frac{\sqrt{X}}{kT_x} \tag{2-9}$$

so that

$$f(\epsilon) = c\left(\exp\left[-\frac{\sqrt{X\epsilon}}{kT_x}\right]\right), \quad \epsilon > X \tag{2-10}$$

$\epsilon < X$. Since $f(\epsilon)$ is now known for $\epsilon > X$, the coupled terms in the collision term of equation (1-2) can be evaluated. If the previous assumptions are used, and $\epsilon^{\frac{1}{2}} f(\epsilon)$ is substituted for $F(\epsilon)$, equation (1-2) eventually becomes

$$\frac{\partial f}{\partial \epsilon} = \frac{-cX}{4\epsilon^{3/2}(kT_x)^2} \int_0^{\epsilon} (\sqrt{y + X}) \exp\left[-\frac{\sqrt{X}\sqrt{y + X}}{kT_x}\right] dy \tag{2-11}$$

where c is the constant of integration in Eq (2-8).

The integral in equation (2-11) can be evaluated, but the resulting expression for $\frac{\partial f}{\partial \epsilon}$ cannot be evaluated in closed form. Therefore, the integral in equation (2-11) will be approximated at $\epsilon \approx X$ and $\epsilon << X$. The two solutions for $f(\epsilon)$ that result from integrating these approximate expressions for $\frac{\partial f}{\partial \epsilon}$ will be matched at the boundary between them.

For $\epsilon \approx X$, the upper limit of the integral in equation (2-11) is set equal to X. Integrating twice leads to

$$f(\epsilon) = c \exp\left[\frac{-X}{kT_x}\right] \frac{X^{3/2}}{\epsilon^{\frac{1}{2}} kT_x} + c_1 \quad , \quad q \le \epsilon \le X \tag{2-12}$$

where c_1 is a constant of integration and q is the boundary

between the two solutions for $\epsilon << X$ and $\epsilon \approx X$.

With the change of variable $u = \frac{\sqrt{X}\sqrt{y + X}}{kT_x}$, equation (2-11) may be rewritten as

$$\frac{\partial f}{\partial \epsilon} = \frac{-c}{2\epsilon^{3/2}} \frac{kT_x}{\sqrt{X}} \int_{\frac{X}{kT_x}}^{\frac{X}{kT_x}\left(1 + \frac{\epsilon}{X}\right)^{\frac{1}{2}}} u^2 e^{-u} du \quad , \quad \epsilon \leq X \qquad (2\text{-}13)$$

For $\epsilon << X$, the upper limit may be approximated by $\frac{X}{kT_x}\left(1 + \frac{\epsilon}{2X}\right)$. If the integral is then evaluated, using $X/kT_x >> 1$, the result is

$$\frac{\partial f}{\partial \epsilon} = \frac{-c \exp\left[\frac{-X}{kT_x}\right]}{2kT_x} \left(\frac{X}{\epsilon}\right)^{3/2} \left\{1 - \exp\left[\frac{-\epsilon}{2kT_x}\right]\right\} , \quad \epsilon \leq q \quad (2\text{-}14)$$

This cannot be readily integrated. However, by using the McLaurin series for the exponential, the equation can be reduced to

$$\frac{\partial f}{\partial \epsilon} = \frac{-c \exp\left[\frac{-X}{kT_x}\right]}{2kT_x} \left(\frac{X}{\epsilon}\right)^{3/2} \sum_{n=1}^{\infty} \left[\frac{-1}{2kT_x}\right]^n \frac{\epsilon^n}{n!(n - \frac{1}{2})} \quad , \quad \epsilon \leq q \qquad (2\text{-}15)$$

For $\epsilon = q$ (the worst case), and $q = kT_x$, a choice which is discussed in Appendix B, the first three terms A_n in the series are

$$A_1 = 1$$
$$A_2 = .0833 \qquad (2\text{-}16)$$
$$A_3 = .00833$$

It should be obvious that retaining the first two terms alone gives excellent results. The resulting equation may be integrated to give

$$f(\epsilon) = \frac{c \exp(-X/kT_x)}{4} \left(\left(\frac{X^{3/2}}{3(kT_x)^3} \right) \epsilon^{3/2} - \left(\frac{2X^{3/2}}{(kT_x)^2} \right) \sqrt{\epsilon} \right)$$
$$+ c_2 \quad , \quad \epsilon \leq q \qquad (2\text{-}17)$$

where c_2 is a constant of integration.

Complete Solution. Since $\frac{F(\epsilon)}{N} d\epsilon$ represents the proportion of the total electron population with energies ϵ to $\epsilon + d\epsilon$, $\int_0^\infty \frac{F(\epsilon)}{N} d\epsilon$ should equal 1. This leads to the normalization condition

$$\int_0^\infty \frac{\epsilon^{\frac{1}{2}} f(\epsilon) d\epsilon}{N} = 1 \qquad (2\text{-}18)$$

Utilizing Eq (2-17), $q = kT_x$, continuity of $f(\epsilon)$, and defining $f(X) = 1$, the following solution is found:

$$f(\epsilon) = \exp\left[\frac{X}{kT_x} \left(1 - \left(\frac{\epsilon}{X} \right)^{\frac{1}{2}} \right) \right] \quad , \quad \epsilon > X$$
$$f(\epsilon) = 1 + \frac{X}{kT_x} \left[\left(\frac{X}{\epsilon} \right)^{\frac{1}{2}} - 1 \right] \quad , \quad kT_x < \epsilon < X \qquad (2\text{-}19)$$

$$f(\epsilon) = 1 + \frac{X}{kT_x}\left[\frac{17}{12}\left(\frac{X}{kT_x}\right)^{\frac{1}{2}} - 1\right] + \frac{X^{3/2}}{4(kT_x)^2}\left[\frac{\epsilon^{3/2}}{3kT_x} - 2\epsilon^{\frac{1}{2}}\right] ,$$

$$\epsilon < kT_x \qquad (2\text{-}19)$$

$$N = X^{3/2}\left[\frac{7}{18} + \frac{X}{3kT_x} + \frac{2kT_x}{X} + \frac{4(kT_x)^2}{X^2} + \frac{4(kT_x)^3}{X^3}\right]$$

By defining a dimensionless variable $u = \frac{\epsilon}{X}$ and a parameter $\alpha = \frac{X}{kT_x}$, the solution can be written in the following form:

$$f(u) = \exp(\alpha(1 - \sqrt{u})) \quad , \quad u > 1$$

$$f(u) = 1 + \alpha(\sqrt{1/u} - 1) \quad , \quad 1/\alpha < u < 1 \qquad (2\text{-}20)$$

$$f(u) = 1 + \alpha\left[\frac{17}{12}\sqrt{\alpha} - 1\right] + \frac{\alpha^2}{4}\left[\alpha u^{3/2} - 2u^{1/2}\right) \quad , \quad 0 < u < \frac{1}{\alpha}$$

$$N = X^{3/2}\left[\frac{7}{18} + \frac{\alpha}{3} + \frac{2}{\alpha} + \frac{4}{\alpha^2} + \frac{4}{\alpha^3}\right]$$

It is important to note that the form of the solution is determined entirely by α. This is discussed in more detail in Chapter III.

Solution for $f(\epsilon)$, Three-Level Case

Now a more complicated case will be considered. The background gas will be assumed to have two excited levels, with thresholds X_1 and X_2, and rate constants R_1 and R_2 above threshold. It will be assumed that $X_1 < (X_2 - X_1)$. This assumption is made for two reasons. First, it approximates fairly well a large number of molecular systems that have one or more vibrational levels at fairly low energies, and then

electronic excitational levels at higher energies. The approximation is especially good if the spacing among the vibrational levels and among the electronic levels is small compared to the spacing between the vibrational levels and the electronic levels. Second, the assumption makes the form of the solution much simpler. It should be noted that this assumption is not strictly necessary for the solution of the problem. However, without this assumption the complexity of the problem increases greatly without concomitant increases in physical understanding.

$\underline{\epsilon > X}$. For both $\epsilon > X_2$ and $X_1 < \epsilon < X_2$ it is straightforward to show that equation (1-2) leads to equations formally identical to the two level case. The resulting solutions are

$$f(\epsilon) = c_2 \exp\left[\frac{-\sqrt{X_2 \epsilon}}{kT_{x2}} \right] , \quad \epsilon > X_2$$

$$f(\epsilon) = c_1 \exp\left[\frac{-\sqrt{X_1 \epsilon}}{kT_{x1}} \right] , \quad X_1 < \epsilon < X_2 \qquad (2\text{-}21)$$

where

$$\frac{\sqrt{X_2}}{kT_{x2}} = \sqrt{\frac{6n_o(R_1 + R_2)}{\dot{\epsilon}}}$$

$$\frac{\sqrt{X_1}}{kT_{x1}} = \sqrt{\frac{6n_o R_1}{\dot{\epsilon}}}$$

It is still necessary to assume $\frac{X_1}{kT_{x1}} >> 1$, $\frac{X_2}{kT_{x2}} >> 1$, $\frac{n_o}{n_{x1}} >> 1$, and $\frac{n_o}{n_{x1}} >> 1$.

$\epsilon < X_1$. It is also straightforward to show that equation (1-2) leads to an equation for $\partial f/\partial \epsilon$ that has a sum of terms, each of which is formally identical within a multiplicative constant to the term in Eq (2-11). The resulting solutions are

$$f(\epsilon) = \frac{c_1}{2} \exp\left[\frac{-X_1}{kT_{x1}}\right] \frac{X_1^{3/2}}{kT_{x1}\sqrt{\epsilon}} + \frac{c_2}{2} \exp\left[\frac{-X_2}{kT_{x2}}\right] \left(\frac{R_1}{R_1 + R_2}\right) \frac{X_2^{3/2}}{kT_{x2}\sqrt{\epsilon}} + c_3 \quad , \quad q < \epsilon < X_1$$

$$f(\epsilon) = \frac{c_1}{8} \exp\left[\frac{-X_1}{kT_{x1}}\right] \left\{ \frac{X_1^{3/2}\,\epsilon^{3/2}}{3(kT_{x1})^3} - \frac{2X_1^{3/2}\sqrt{\epsilon}}{(kT_{x1})^2} \right\} + \frac{c_2}{8} \exp\left[\frac{-X_2}{kT_{x2}}\right] \frac{R_1}{(R_1 + R_2)} \left\{ \frac{X_2^{3/2}\,\epsilon^{3/2}}{3(kT_{x2})^3} - \frac{2X_2^{3/2}\sqrt{\epsilon}}{(kT_{x2})^2} \right\} + c_4 \quad , \quad \epsilon < q \qquad (2\text{-}22)$$

Complete Three-Level Solution. By defining $f(X_2) = 1$, using continuity of $f(\epsilon)$ and Eq (2-18), and choosing $q = kT_{x1}$ (this choice is discussed in Appendix B), the following expressions for $f(\epsilon)$ and N are developed for the three-level model.

$$f(\epsilon) = \exp\left[\frac{X_2}{kT_{x2}}\left(1 - \sqrt{\frac{\epsilon}{X_2}}\right)\right] \quad , \quad X_2 < \epsilon$$

$$f(\epsilon) = \exp\left[\frac{\sqrt{X_1 X_2}}{kT_{x1}}\left(1 - \sqrt{\frac{\epsilon}{X_2}}\right)\right] \quad , \quad X_1 < \epsilon < X_2$$

$$f(\epsilon) = \exp\left[\frac{\sqrt{X_1X_2} - X_1}{kT_{x1}}\right] + \frac{1}{2}\left(\frac{1}{\sqrt{\epsilon}} - \frac{1}{\sqrt{X_1}}\right)\left\{\exp\left[\frac{\sqrt{X_1X_2} - X_1}{kT_{x1}}\right] \frac{X_1^{3/2}}{kT_{x1}}\right.$$

$$\left. + \frac{R_1}{(R_1 + R_2)} \frac{X_2^{3/2}}{kT_{x2}}\right\} \quad , \quad kT_{x1} < \epsilon < X_1$$

$$f(\epsilon) = \exp\left[\frac{\sqrt{X_1X_2} - X_1}{kT_{x1}}\right] \frac{X_1^{3/2}}{(kT_{x1})^2}\left(\frac{\epsilon^{3/2}}{24kT_{x1}} - \sqrt{\frac{\epsilon}{4}}\right)$$

$$+ \frac{R_1}{(R_1 + R_2)} \frac{X_2^{3/2}}{(kT_{x2})^2}\left(\frac{\epsilon^{3/2}}{24kT_{x2}} - \sqrt{\frac{\epsilon}{4}}\right)$$

$$+ \exp\left[\frac{\sqrt{X_1X_2} - X_1}{kT_{x1}}\right]\left(\frac{17}{24}\left(\frac{X_1}{kT_{x1}}\right)^{3/2} - \frac{X_1}{2kT_{x1}} + 1\right)$$

$$+ \frac{R_1X_2^{3/2}}{2(R_1 + R_2)}\left\{\frac{(kT_{x1})^{1/2}}{2(kT_{x2})^2} - \frac{(kT_{x1})^{3/2}}{12(kT_{x2})^3} + \frac{1}{kT_{x2}(kT_{x1})^{1/2}}\right.$$

$$\left. - \frac{1}{kT_{x2}(X_1)^{1/2}}\right\} \quad , \quad \epsilon < kT_{x1} \qquad (2\text{-}23)$$

$$N = 2\left\{\sqrt{X_2}(kT_{x2}) + \frac{2(kT_{x2})^2}{\sqrt{X_2}} + \frac{2(kT_{x2})^3}{X_2^{3/2}} - \frac{X_2(kT_{x1})}{\sqrt{X_1}} - \frac{2(kT_{x1})^2\sqrt{X_2}}{X_1}\right.$$

$$\left. - \frac{2(kT_{x1})^3}{X_1^{3/2}}\right\} + \exp\left[\frac{\sqrt{X_1X_2} - X_1}{kT_{x1}}\right]\left\{2\sqrt{X_1}kT_{x1} + \frac{4(kT_{x1})^2}{\sqrt{X_1}}\right.$$

$$\left. + \frac{4(kT_{x1})^3}{X_1^{3/2}} + \frac{X_1^{5/2}}{6kT_{x1}} + \frac{19X_1^{3/2}}{36}\right\} + \frac{R_1}{6(R_1 + R_2)} \frac{X_2}{kT_{x2}}\left\{X_1 - kT_{x1}\right.$$

$$\left. - \frac{(kT_{x1})^3}{12(kT_{x2})^2} + \frac{(kT_{x1})^2}{4kT_{x2}}\right\}$$

Extension of the Solution

More Levels ($X_1 < X_2 - X_1$). Although the algebra would become quite involved, the extension of this model to four or more levels would be quite straightforward, as long as the appropriate assumptions about $\frac{X}{kT_x}$ and $\frac{n_o}{n_x}$ can still be made. As long as ϵ is greater than some threshold energy X_n, $f(\epsilon)$ will have the form of equation (2-20), with R replaced by a sum of R_β over all states β with threshold energies less than or equal to X_n. For β less than any threshold energy, the differential equation for $\partial f/\partial \epsilon$ can be reduced to the form of a sum of terms, each of which is formally identical within a multiplicative constant to the terms in equation (2-11). This results in forms similar to equation (2-23), but even more complex.

$X_1 > (X_2 - X_1)$. (See Figure 3).

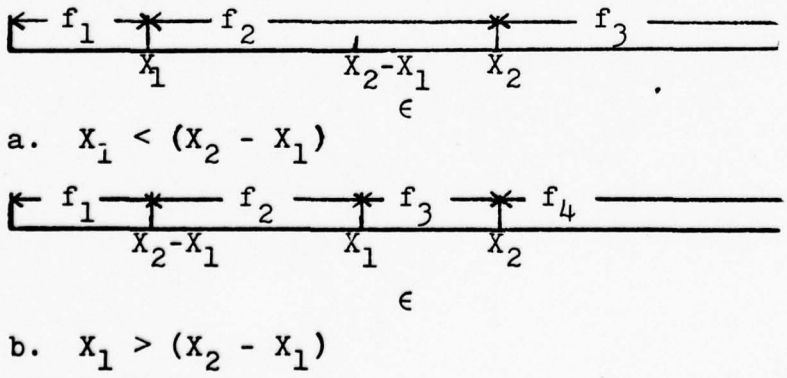

a. $X_1 < (X_2 - X_1)$

b. $X_1 > (X_2 - X_1)$

Figure 3. Comparisen of threshold energy relationships

The extension in this case would be fairly straightforward. The distribution function at some energy ϵ is determined by the rate electrons are lost at that energy due to inelastic collisions, if those collisions are possible at ϵ. This is the process applicable for f_2 and f_3 in Fig 3a, and f_3 and f_4 in Fig 3b. If ϵ is less than all the threshold energies, then inelastic collisions cannot take place. In this case the distribution at ϵ is determined by the rate at which electrons are gained from inelastic collisions at energies $\epsilon + X_\beta$, which is proportional to $f(\epsilon + X_\beta)$. This is the process applicable for f_1 in Fig 3a, and f_1 and f_2 in Fig 3b. In Fig 3a, $f(\epsilon + X_1)$ has the same form for any energy ϵ in the range $0 < \epsilon < X_1$. As a result, one differential equation is valid for the entire range. In Fig 3b, $f(\epsilon + X_1)$ changes form as ϵ goes from $0 < \epsilon < (X_2 - X_1)$ to $X_2 - X_1 < \epsilon < X_1$ (or as ϵ goes from f_1 to f_2). As a result, two differential equations are necessary for the range $0 < \epsilon < X_1$. This does not cause any fundamental difficulties, but does lead to a much more complicated expression for $f(\epsilon)$.

III Analysis and Conclusion

General Considerations

The analytic two-level solution has two parameters; X and kT_x. However, it is possible to express $f(\epsilon)$ in terms of $\frac{X}{kT_x}$ and the dimensionless parameter $u = \frac{\epsilon}{X}$. As a result, it is more appropriate to characterize the various solutions by the corresponding values of X/kT_x; all the solutions presented here are so identified.

Much the same situation exists for the three-level case, except that the parameters are now X_1, X_2, kT_{x1}, kT_{x2}, and $\frac{R_1}{R_1 + R_2}$. With this many parameters, it would be impractical to try to represent all possible combinations, and there has been no attempt to do so here.

All the cross-sections used for comparison of the analytic solution to realistic gases are from Kiefer (Ref 6). Since each cross-section will be identified at the time it is introduced, there will be no further citations of the cross-section source. All numerical calculations were done with the program NGB, as discussed in Appendix C.

Criteria for Evaluation

A discussion of the criteria used to evaluate the analytic solutions developed in this thesis would be in order at this time. In general, analytic models cannot describe physical situations as complicated as the one involved here as accurately as numerical solutions. Therefore, it would

be inappropriate to use exact agreement with the numerical solution as a general criterion for evaluating the numerical solution, although such agreement certainly adds support to the validity of both the numerical and analytic solutions.

More appropriate criteria would be those that measure the insight the analytic model gives into the physical situation. For instance, it is more important to be able to demonstrate the dependence of f on ϵ than to produce hard numbers. Based on this principle, the following criteria were used to evaluate the validity and utility of the analytic solutions:

1. Does the analytic solution dependence on electron energy agree with that of the numerical solution, within the limits of the numerical solution?
2. Can the analytic solution be used to predict the scaling of physical parameters in a meaningful fashion?

Obviously, the first condition is met for those cases where the two solutions are essentially indistinguishable, but even if there are differences between the two solutions, this condition can still be met if the two solutions have similar slopes at the same energy (See Fig 9).

As long as the first condition is met, the analytic solution can be considered valid. It can be considered useful if the second condition is met. The success of this model in meeting the second criterion will be discussed later in this chapter.

Of course, it is possible that an analytic model will

demonstrate other results in excess of the criteria listed above. Such serendipitous results may increase the utility of such a model, but the lack of them does not invalidate it.

Theoretical Cross-Sections

Two-Level Model. Figures 4,5,6,and 7 show the analytic and numerical solutions for values of X/kT_x of 10, 20, 30, and 100. The cross-sections used were calculated to produce R's constant above threshold. The background gas contained no excited atoms and the numerical calculations included only the effects of heating and inelastic collisions.

Several points should be made. First, the apparent discrepancy at the extreme high energy end of the energy axis is purely a result of NGB. NGB always conserves the total electron density. As a result, electrons being driven up the energy axis by heating must eventually stop at the upper boundary. This causes the increase in $f(\epsilon)$ at the upper end of the axis. (In some cases the entire energy axis used in NGB is not depicted, in which case this discrepancy is absent).

Second, there is a discrepancy at the low-energy end of the energy axis. This is also a result of the finite differencing used in NGB. The behavior of $f(\epsilon)$ for $\epsilon \approx 0$ is strongly influenced by $f(\epsilon + X)$. The distribution function drops very rapidly just above X. If the resolution of NGB is larger than the interval over which $f(\epsilon)$ drops, it will be unable to accurately describe the behavior at $\epsilon \approx X$,

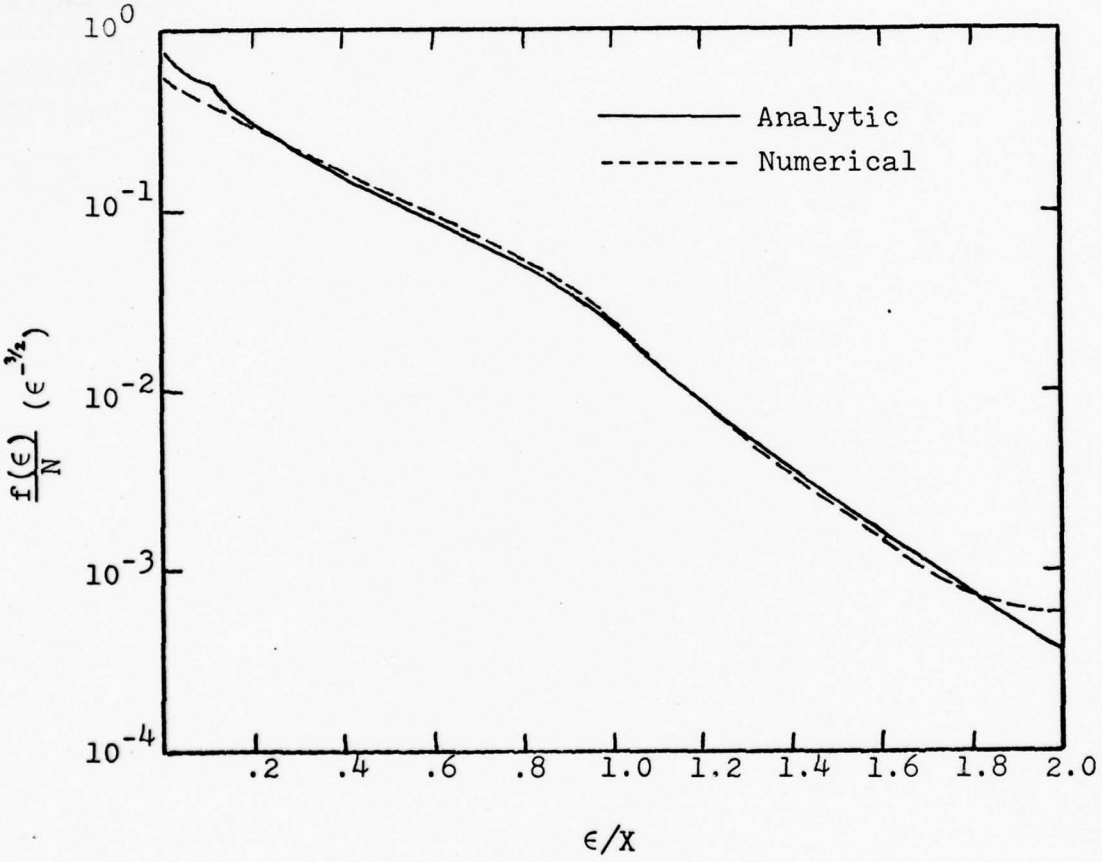

Figure 4. Ideal Two Level System, $\frac{X}{kT_x} = 10$

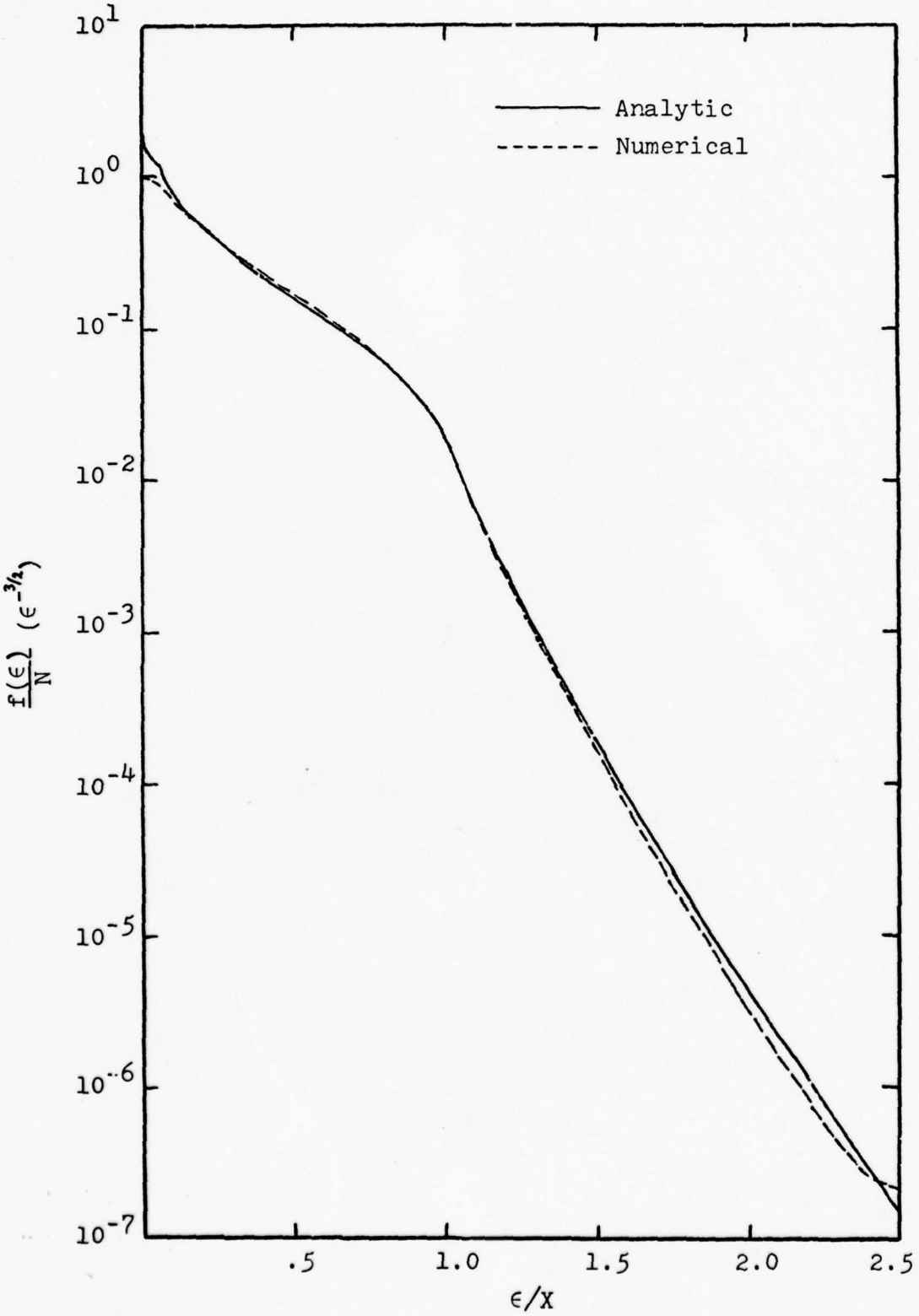

Figure 5. Ideal Two Level System, $\frac{X}{kT_x} = 20$

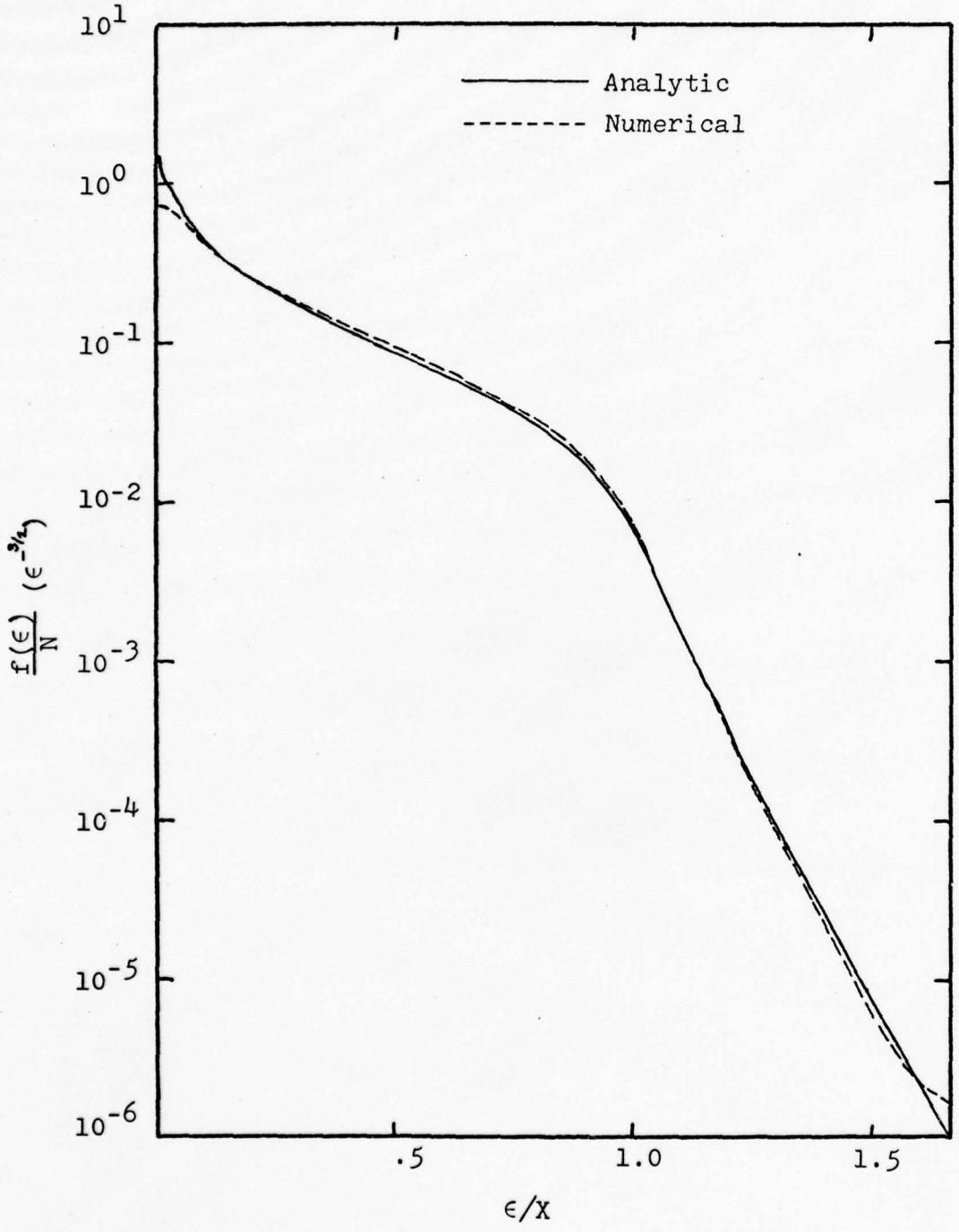

Figure 6. Ideal Two Level System, $\frac{X}{kT_x} = 30$

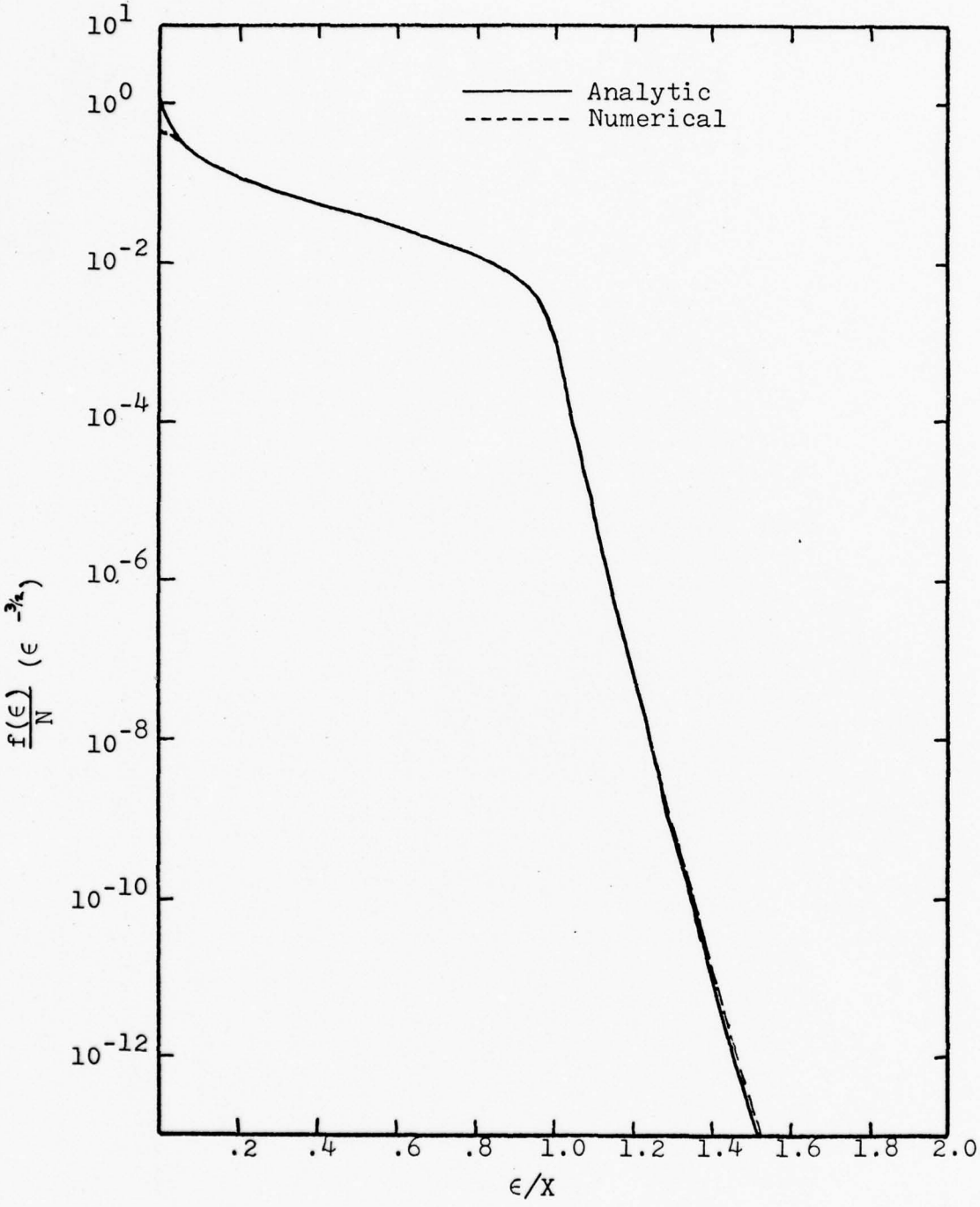

Figure 7. Ideal Two Level System, $X/kT_x = 100$

and also at $\epsilon \approx 0$ as a result of the strong coupling. Increasing the resolution in NGB would improve the agreement between the analytic and numerical solutions.

Figure 8 shows two numerical solutions and the analytic solution for $X/kT_x = 15$. Notice that as the energy resolution increases, the discrepancy at the low end of the energy axis decreases. Note also that as the upper end of the energy axis moves down, the discrepancy at that end moves down also. This clearly demonstrates that the discrepancy at that end is a result of NGB and does not reflect physical reality.

Finally, it is apparent that the numerical and analytic solutions agree very well, especially for values of $\frac{X}{kT_x}$ greater than ~ 15 .

Three-Level Model. Figure 9 shows analytic and numerical solutions of an idealized three level system. The numerical and analytic solutions do not agree as well for this case as for the various two-level cases, especially for $\epsilon \approx X_1$. However, note that the scaling for $\epsilon > X_1$ is still very good, as evidenced by the fact that the two curves have very similar slopes. In addition, a comparison of the average pumping rate for the second level, given by

$$\langle R_2 \rangle = \int_0^\infty R_2(\epsilon) F(\epsilon) d\epsilon \qquad (3\text{-}1)$$

results in a value of $R_2 = 6.9 \times 10^{-18}$ cm^3/sec for the analytic case, versus 3.6×10^{-18} for the numerical (Equation

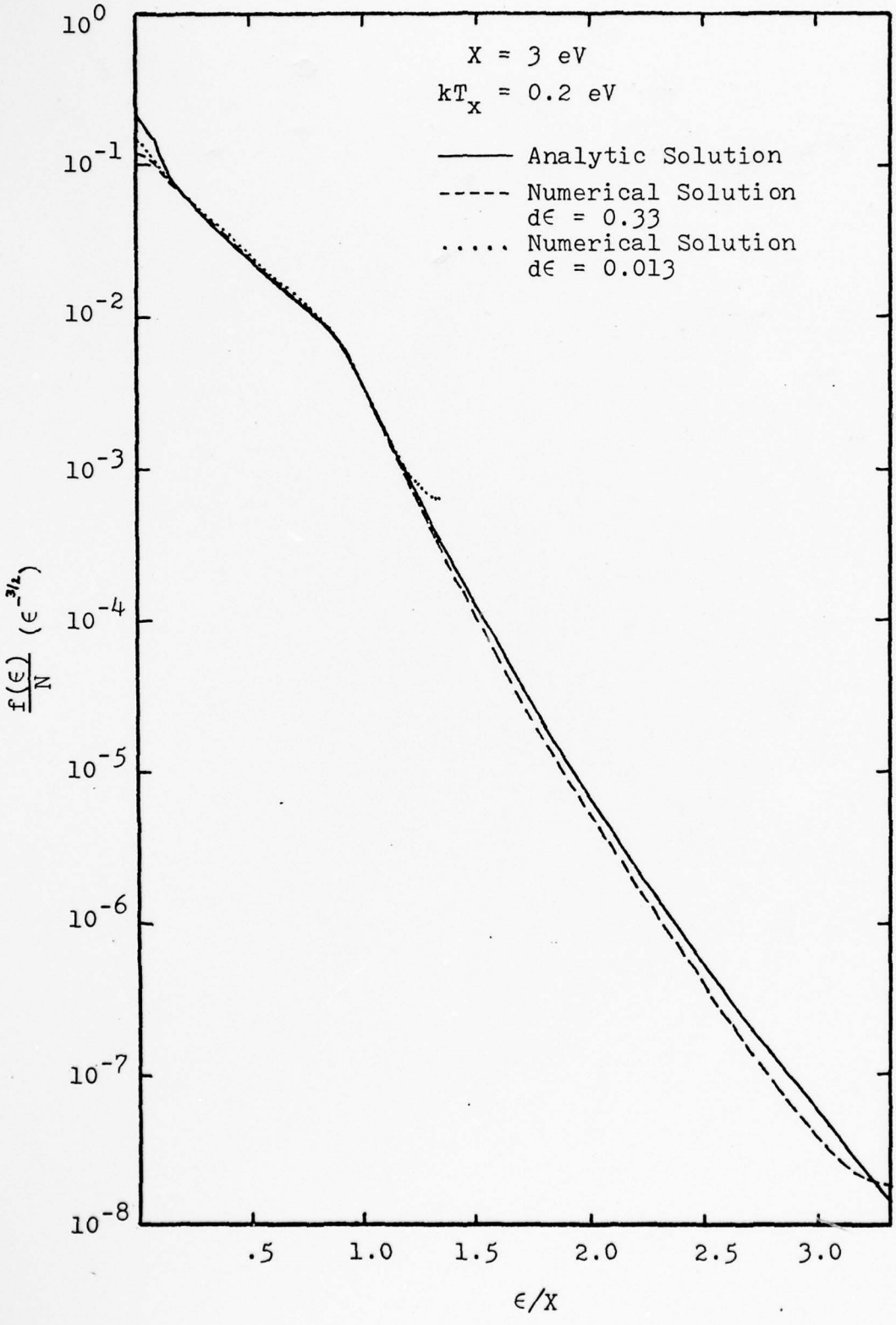

Figure 8. Demonstration of Finite Differencing Discrepancies

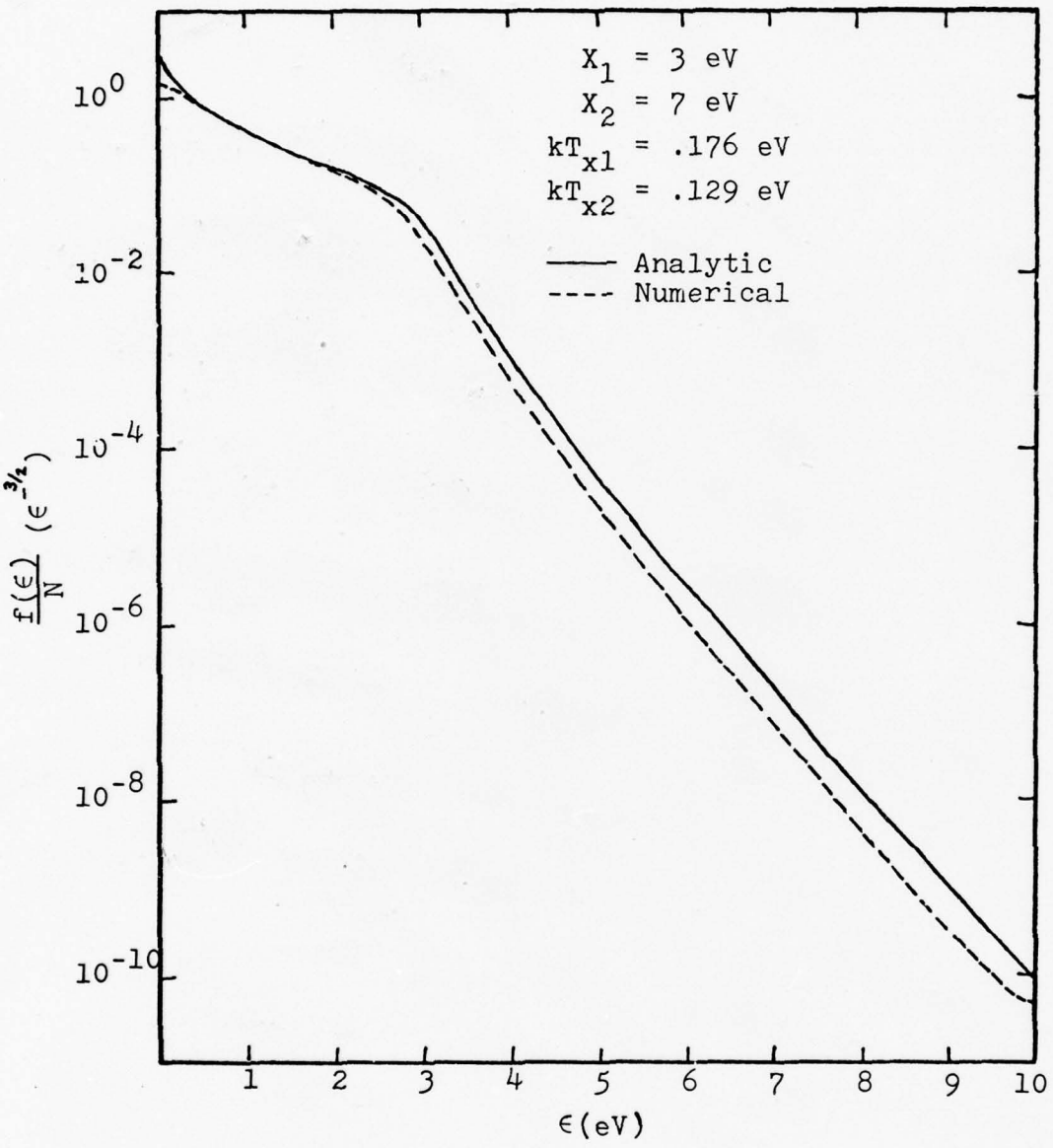

Figure 9. Ideal Three Level System

(3-6) gives $\langle R_2 \rangle$ more explicitly). As described in Nielsen's unpublished paper, the pumping rates of the higher levels can be very sensitive to the width of the energy bins. Since $f(\epsilon)$ drops off rapidly within a range $\sim kT_x$ above threshold, most of the electrons that lose energy do so with a range $\sim kT_x$ above that threshold. These electrons are spread throughout the first energy bin, if that bin is wider than kT_x. This error in the electron density in energy space can cause errors throughout the energy axis, due to the strong coupling of the Boltzmann equation. In the example shown in Figure 9, $d\epsilon$ was .1 eV , while kT_{x1} was .129 eV, and kT_{x2}, .176 eV. With $d\epsilon$ so close to kT_{x1}, it is difficult to say which of the two average rates is more accurate; computer limitations made it impractical to use higher resolution on the energy axis. In any case, the agreement is certainly close enough to be useful in predicting realistic reaction rates, as will be seen later.

Note that, unless $\dot{\epsilon}$ is very large, $\langle R_1 \rangle \gg \langle R_2 \rangle$. This means that, as for the two-level case, conservation of energy implies

$$\langle R_1 \rangle n_o = \frac{\epsilon}{X} \qquad (3\text{-}2)$$

independent of the exact form of the distribution function, as long as $\langle R_1 \rangle \gg \langle R_2 \rangle$. For this reason $\langle R \rangle$ is not a useful test for the two-level model, nor is $\langle R_1 \rangle$ for the three level model.

Realistic Cross-Sections

Two-Level Model. Figures 10, 11, and 12 show comparisons of the analytic and numerical solutions using realistic cross-sections. Figure 10 is based on the cross-sections for the lowest electronic state for N_2. Figure 11 is based on the second electronic state for N_2. Figure 12 is based on the second electronic state for Ar. Several different methods of matching the analytic cross-sections and thresholds to the realistic ones were used. The method finally used was to choose an analytic R of one-half the maximum reaction rate for the real cross-section, where the reaction rate is given by

$$R(\epsilon) = \left(\frac{\epsilon}{2m}\right)^{\frac{1}{2}} \sigma(\epsilon) \qquad (3\text{-}3)$$

where m is the electron mass

σ is the inelastic collision cross-section (Ref 13: 2349).

The threshold was chosen equal to the energy lost by the electron upon collision. This method of matching was used primarily because it worked. This point will be discussed in more detail later.

From Figures 10, 11, and 12 it seems that the analytic and realistic solutions match fairly well, except at the high energy end of Figures 10 and 12. This discrepancy is caused by the exact behavior of the realistic cross-sections. The analytic model assumes that there is a finite cross-section for all energies above the threshold. In this case, however, the real cross-se tions go to zero. As a result

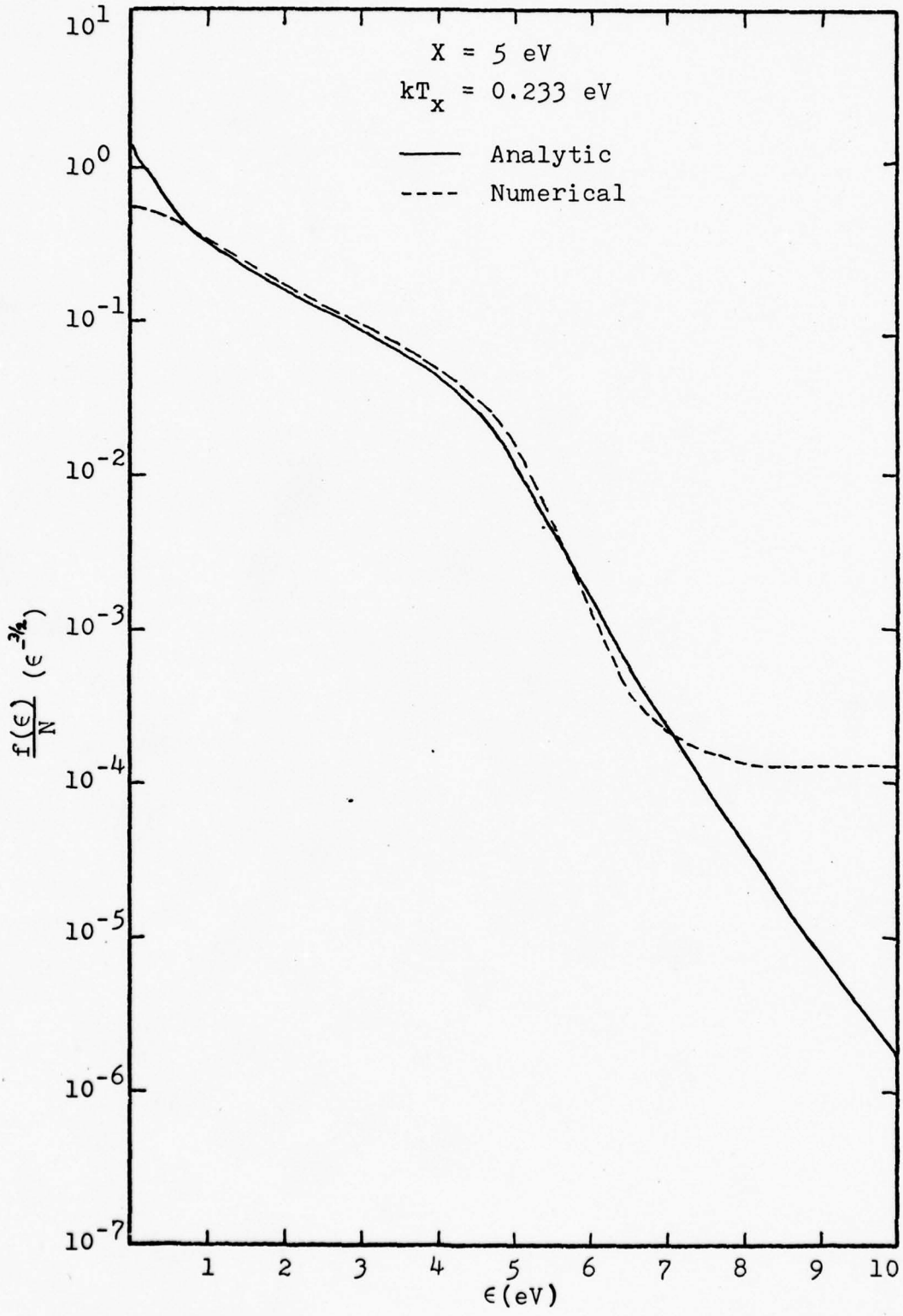

Figure 10. Two Level System, El Level of N_2

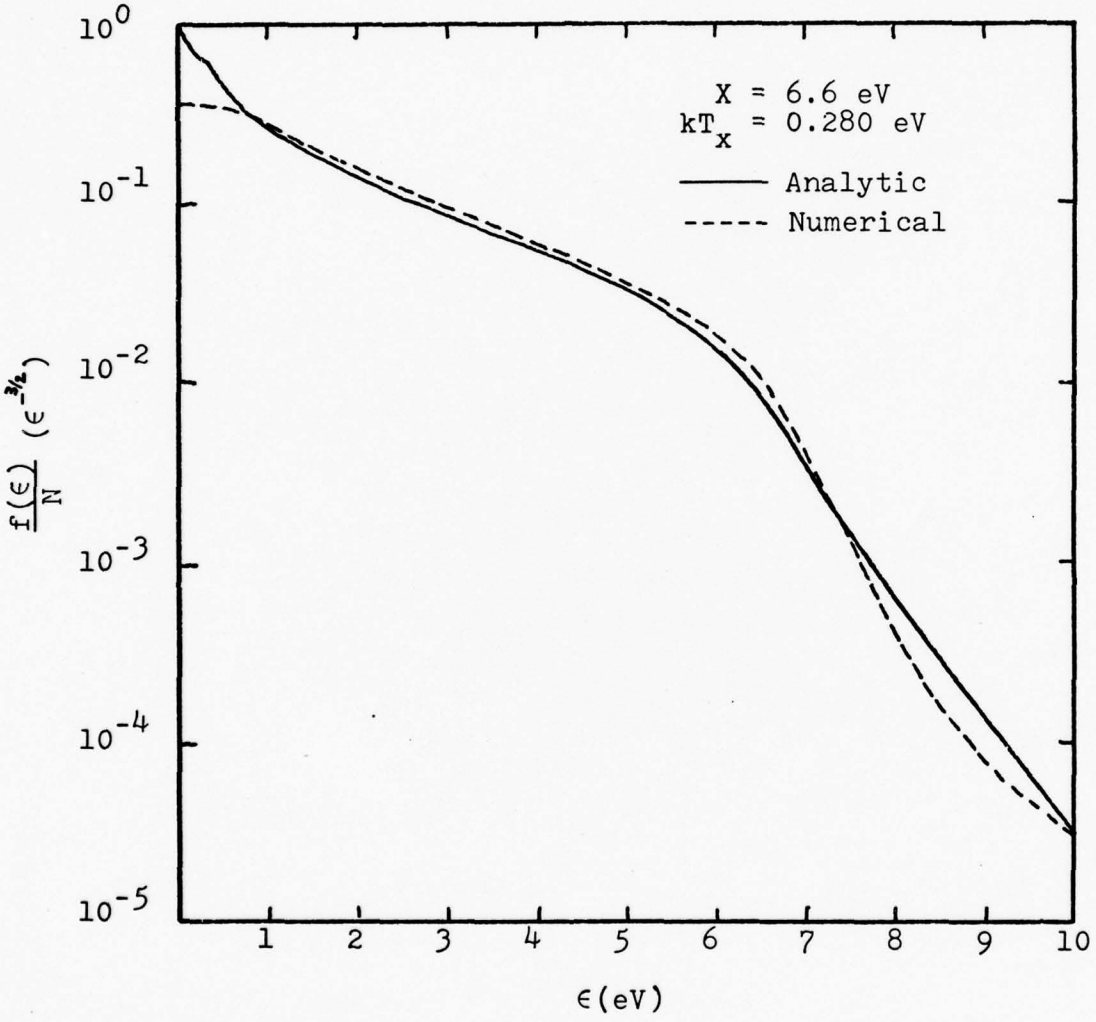

Figure 11. Two Level System, E2 Level of N_2

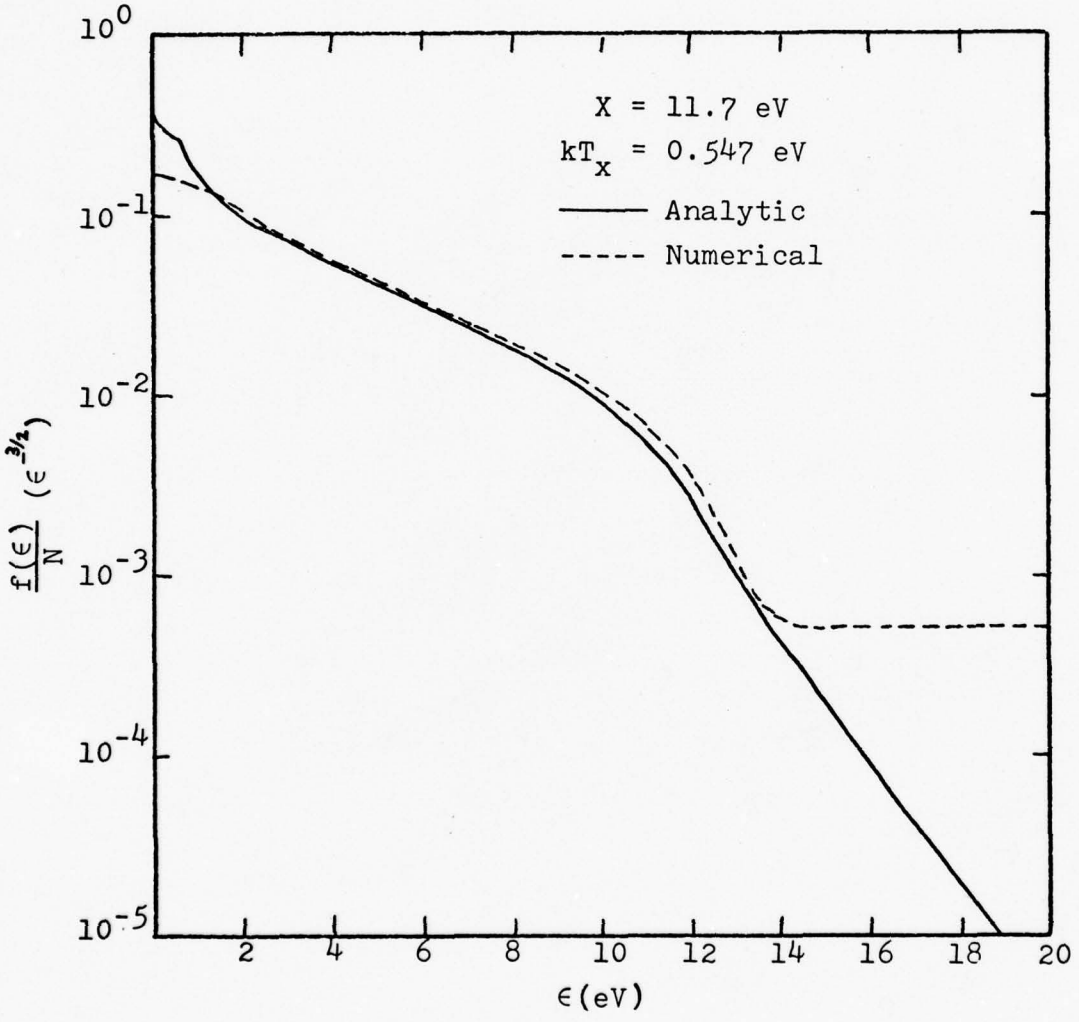

Figure 12. Two Level System,

E2 Level in Argon

(since elastic collisions are excluded), there is no mechanism to allow the electrons to lose energy, and the distribution approaches an infinite-temperature Maxwellian distribution.

Three-Level Model. Figures 13, 14, and 15 compare the numerical and analytic results for three different cases. Figure 13 is based on the first and fourth electronic levels on N_2. Figure 14 is based on the second and fifth electronic levels of N_2. Figure 15 is based on the first and fifth levels on N_2. In all cases the analytic reaction rates were chosen to be one half the maximum realistic rates; the thresholds were chosen equal to the energy loss for each transition. The agreement in Figures 13 and 14 is fairly close; however, the agreement in Figure 15 is poor. The analytic and numerical pumping rates for the second excited level for Figure 13 are 2.78×10^{-11} cm^3/sec and 6.42×10^{-11} cm^3/sec, respectively. For Figure 14, the values are 4.42×10^{-12} cm^3/sec and 4.53×10^{-12} cm^3/sec, respectively. For Figure 15, the values are 8.49×10^{-15} cm^3/sec and 1.14×10^{-11} cm^3/sec, respectively. Again, the results in Figures 13 and 14 agree well; those in Figure 15 do not. The discrepancy is caused by an effect similar to that just discussed for Figures 10 and 12. For the data depicted in Figure 15, there is a region between X_1 and X_2 where all the cross-sections are zero. As a result, any electron that reaches this region cannot lose energy by exciting a background atom. Instead, it must keep increasing in energy until it reaches X_2. This causes $f(\epsilon)$ to be

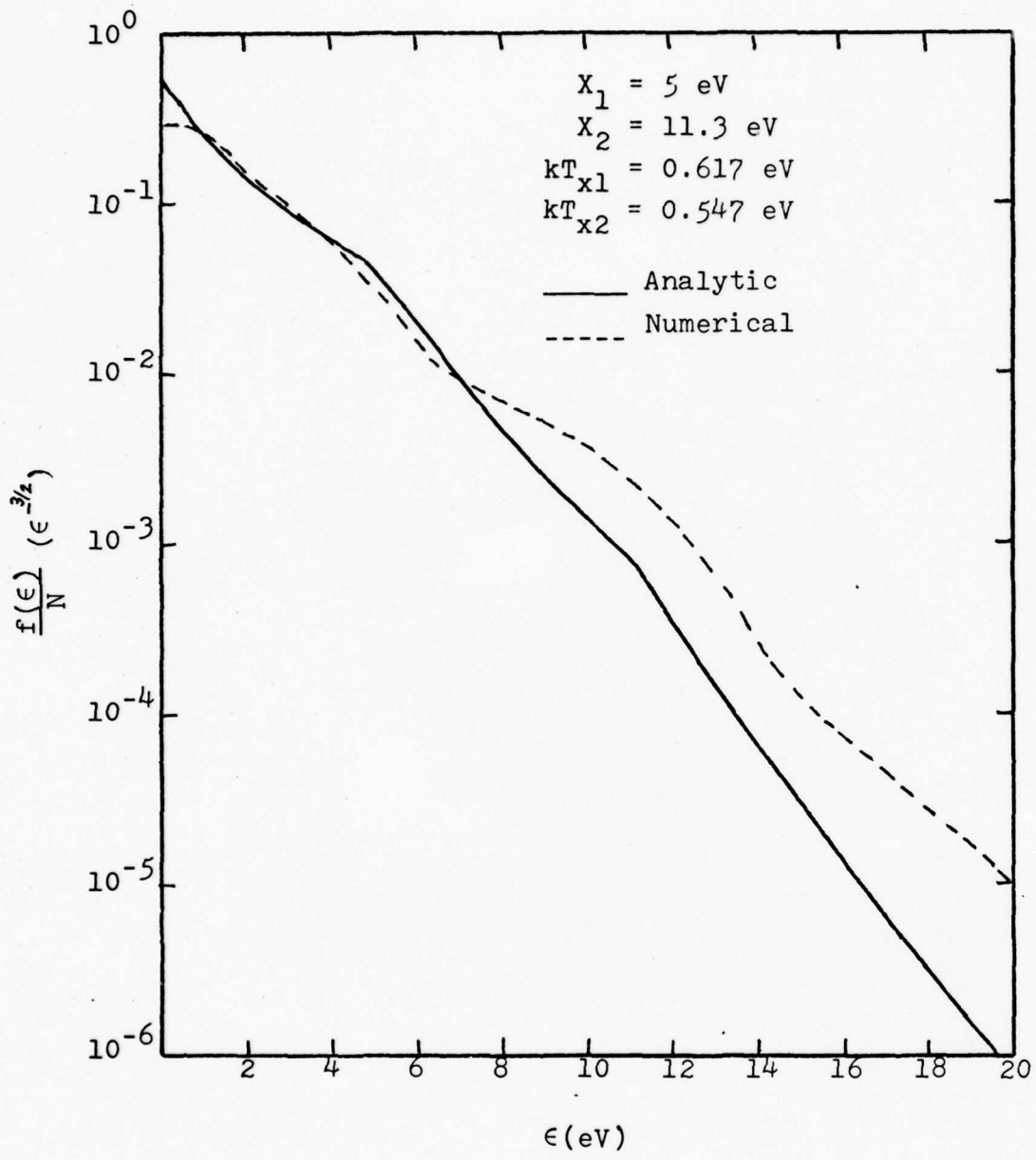

Figure 13. Three Level System,
E1 and E4 Levels of N_2

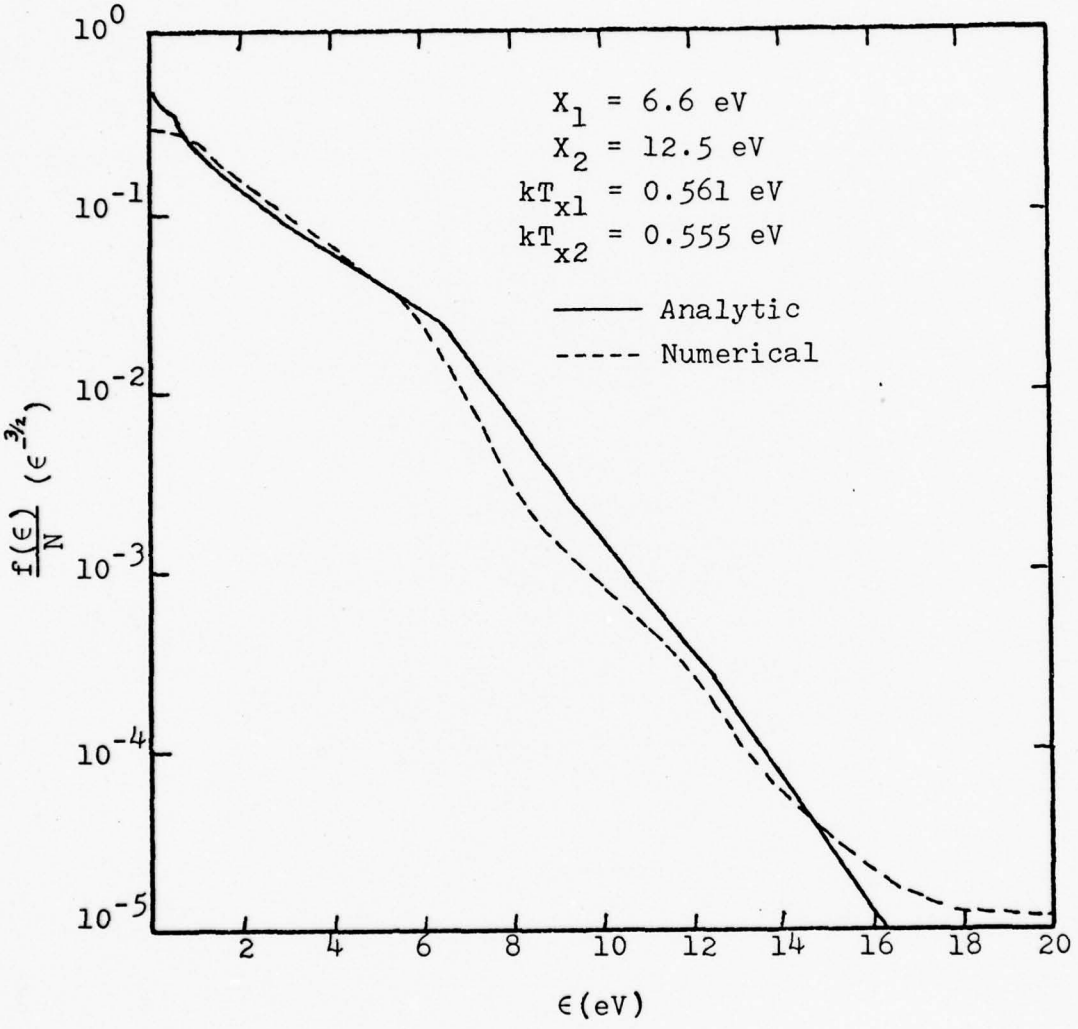

Figure 14. Three Level System,

E2 and E5 Levels of N_2

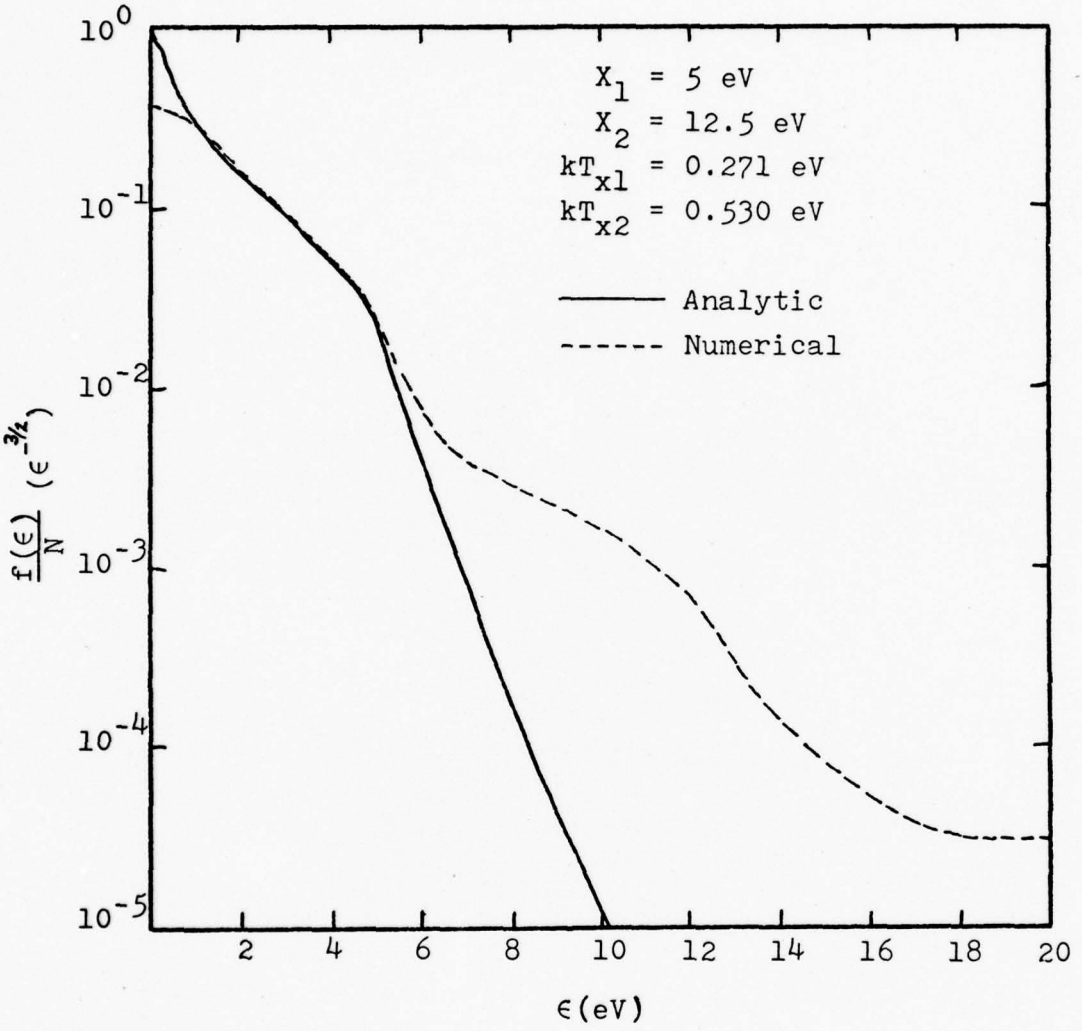

Figure 15. Three Level System,

E1 and E5 Levels of N_2

much higher in this region than the analytic model predicts. In the conclusions, a method to correct this discrepancy will be discussed. On the other hand, if the two cross-section profiles overlap, the process described above does not occur, and the result agrees with the analytic model. Although this effect limits the number of real cases which can be described by this model, it does not significantly reduce the effectiveness of the model in meeting the criteria discussed earlier, especially since it is possible to predict a priori when this effect will occur.

Modeling a Multi-Level System. Figure 16 shows a comparison between a five-level system and a three-level analytic model. The five-level system is intended to represent a system with characteristics similar to a real system. The system uses cross-sections for the sixth and seventh vibrational and the first and second electronic levels of CO. Program limitations in NGB made it impractical to use all seven vibrational levels. These limitations could be easily removed, if necessary. However, in this particular case, such modification would not be worth the effort involved. For R_1, the analytic model used one half the average of the maximum rates for the V6 and V7 levels. For R_2, the analytic model used one half the average of the maximum rates for the E1 and E2 levels. For X_1, the analytic model uses the average of the energy losses for the V6 and V7 transitions. For X_2, the analytic model uses the average of the energy losses for the E1 and E2 levels. The numerical results for the pumping rates for E1 and E2 are

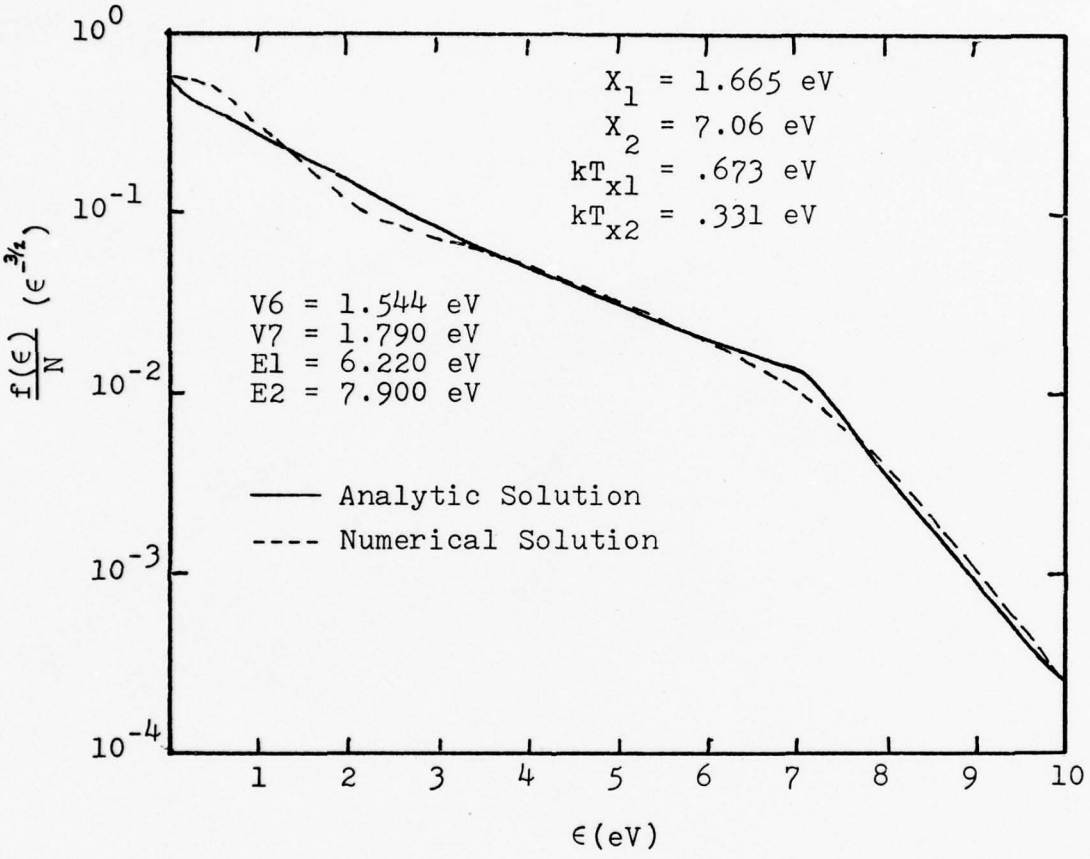

Figure 16. Five Level System, V6, V7, E1, and E2 Levels in CO

$\langle R_{E1} \rangle = 2.07 \times 10^{-10}$ cm^3/sec and $\langle R_{E2} \rangle = 1.34 \times 10^{-11}$ cm^3/sec. The analytic rates for E1 and E2 are given by Equation (3-6) with X_2 and R_2 replaced by X_{E1}, X_{E2}, R_{E1}, and R_{E2}, as appropriate, and with X_1, and R_1 as described above. The results are $\langle R_{E1} \rangle = 2.6 \times 10^{-10}$ cm^3/sec and $\langle R_{E2} \rangle = 2.6 \times 10^{-9}$ cm^3/sec . The poor agreement for the E2 level is not surprising; the analytic model assumes the level involved is well-separated from any lower thresholds, a condition which certainly does not hold. Since $f(\epsilon)$ drops rapidly above threshold, the presence of a higher threshold is not as significant. The close agreement for the E1 level and for the distribution function itself indicates that the analytic solution would be useful for modeling cases similar to this one.

Superelastic Collisions. Figure 17 shows the result of a numerical and analytic comparison used to investigate the validity of neglecting superelastic collisions. The analytic model used a value of X/kT_x of 25. The numerical calculations used idealized reaction rates constant above $X = 5$ eV . According to the expression developed in Appendix A (Eq (A-11)) superelastic collisions should be negligible as long as $n_o/n_x \gg 3.1 \times 10^4$. The numerical results shown had values of n_o/n_x of 10^7, 10^5, and 10^3 . Values of n_o/n_x greater than 10^7 produced results indistinguishible for the result with $n_o/n_x = 10^7$. As can be seen, the result starts to change for $n_o/n_x = 10^5$. For $n_o/n_x = 10^3$, the numerical solution has values much higher than the analytic at high energies, and lower values at low energies. This is

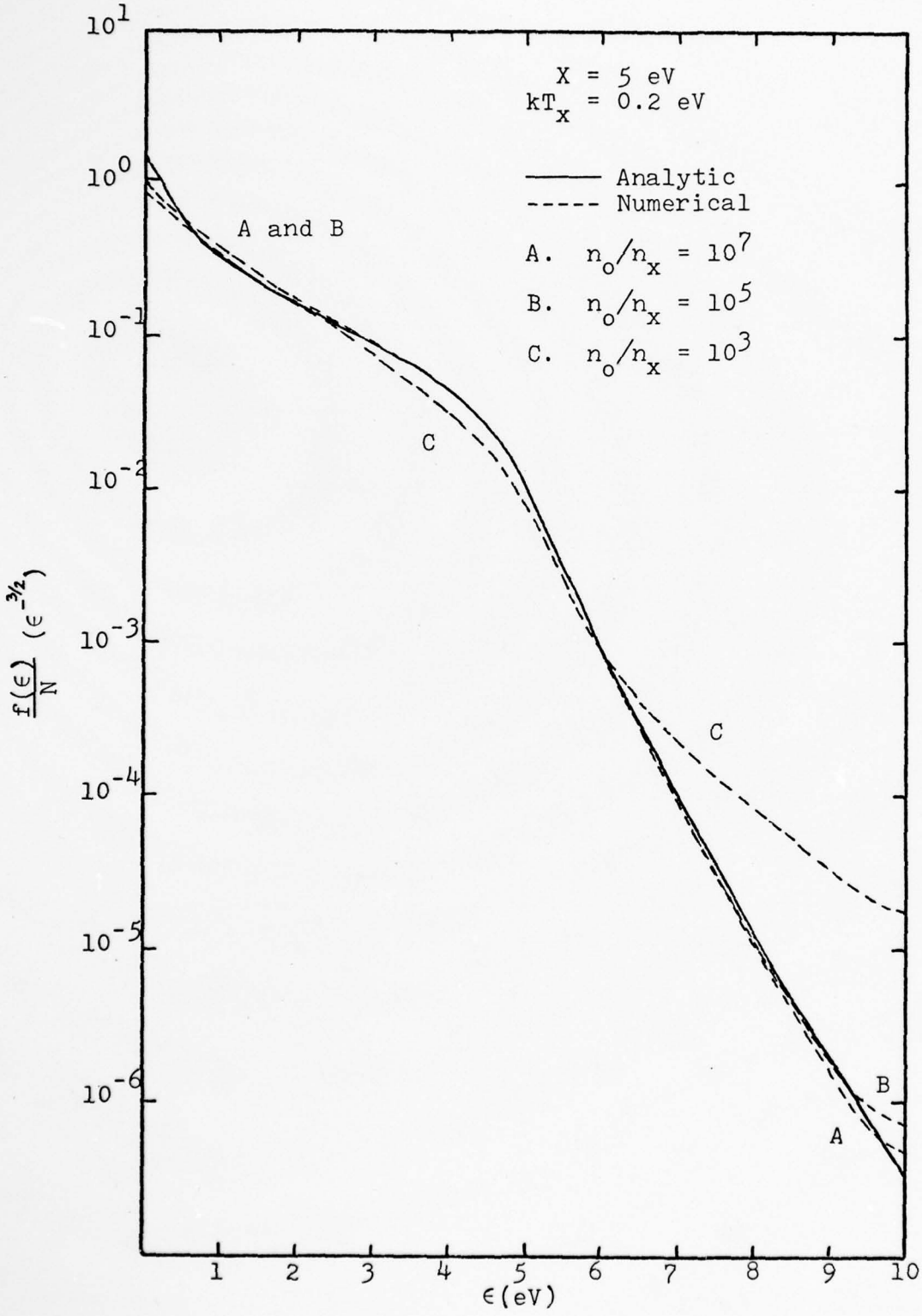

Figure 17. Effect of Superelastic Collisions

exactly the expected result. Superelastic collisions act to transfer electrons from low energies to higher energies; if this transfer involves significant numbers of electrons, the effect is exactly that produced by NGB. Note that the threshold for this effect to become significant agrees very well with that predicted by Eq (A-11).

Conclusions

For a system composed of an electron gas in the presence of background particles capable of being excited internally by the electrons, the form of the electron distribution function depends strongly on the parameters of the form

$$\frac{X}{kT_x} = \sqrt{\frac{6n_o RX}{\dot{\epsilon}}} \tag{3-4}$$

where n_o is the background gas particle density
R is the average reaction rate
X is the excitation threshold
$\dot{\epsilon}$ is the average electron heating rate (per electron)

as long as $\frac{X}{kT_x} \gtrsim 10$ and elastic and superelastic collisions can be ignored.

For heating produced by a uniform non-time-varying electric field, this result reduces to

$$\frac{kT_x}{X} = \frac{E}{n_o}\sqrt{\frac{e^2}{6RXm\nu}} \tag{3-5}$$

where E is the magnitude of the electric field
e is the electron charge
m is the electron mass

ν is the average electron-background particle collision frequency

For typical systems, $\frac{X}{kT_x} >> 1$ implies $\frac{E}{n_o} << 10^{-15}$ Vcm^2 . For laser media under such circumstances, if the excited particle density is low enough that superelastic collisions can be ignored, and if the background gas can be approximated as having two excited levels, the electron pumping to the second level is given by

$$\langle R_2 \rangle = \frac{2\left[\frac{E}{n_o}\right]^2 \frac{R_2 X_2 e^2 n_o}{m\nu} \sqrt{\frac{X_1}{R_1(R_1 + R_2)}}}{\exp\left[\frac{\sqrt{X_1 X_2} - X_1}{\frac{E}{n_o}\sqrt{\frac{X_1 e^2}{6R_1 m\nu}}}\right] X_1^{3/2} + \sqrt{\frac{R_1}{R_1 + R_2}}\, X_2^{3/2} X_1} \qquad (3\text{-}6)$$

where use has been made of $\frac{X}{kT_x} >> 1$ and $X_2 > X_1$.

The importance of the parameter X/kT_x and the manner in which it affects the distribution function indicates that, for a numerical solution to be valid, it must have a resolution much better than kT_x; for example, $kT_x/d\epsilon > 10$.

It is difficult to compare this conclusion with published results, as very few authors give the resolution used in their numerical results. It is interesting to compare with the results that are available. Rockwood decreased the energy difference in his method until further reductions had no effect on the result. The energy difference $d\epsilon$ chosen in this manner was 0.01 eV. Although it is not possible to cal-

culate kT_x exactly from his data, it would be close to 0.005 eV, which certainly is of the same order as $d\epsilon$. (Ref 13) Nielsen et alia, in their work on laser induced breakdown, used the photon energy of the laser photon as $d\epsilon$. In their CO_2 laser breakdown studies, $d\epsilon$ = .1 eV , and $kT_x \approx$ .05 eV (Ref 10). Again the agreement is fairly good. However, in the ruby laser breakdown studies, $d\epsilon$ = 1.7 eV , and kT_x .01 eV . These results seem to invalidate either their results or the analytic model. However, note that the analytic model, by its choice of form of the Boltzmann equation, assumes a continuous heating process. This is completely valid for a D/C field, as was used in Rockwoods research, and is a very good approximation for the CO_2 laser in helium, where the absorbed photons have energies of 0.1 eV and the first threshold is $\sim$ 20 eV . But for a ruby laser in deuterium, where the photon energy is $\simeq$ 1.7 eV , and the first threshold is still $\sim$ 20 eV , it is difficult to justify the continuous heating model.

For physical situations where the assumptions the analytic model is based on are accurate, the analytic model describes physical reality fairly well. In particular, it is necessary that $\dot{\epsilon}$ be low enough for the assumption $\frac{X}{kT_x} >> 1$; that n_* be small enough that superelastic collisions can be ignored; that n_e be low enough that electron-electron interactions can be ignored; and that the heating effect be continuous in energy space. Based on agreement between the analytic and numerical solutions discussed previously, the

final solution is apparently insensitive to the exact form of $R(\epsilon)$, as long as $R(\epsilon) \neq 0$ for $\epsilon > X$. As a result, it is not necessary for $R(\epsilon)$ to closely approximate a constant value.

The analytic two-level solution models realistic distribution functions based on the two-level systems well, especially if $R(\epsilon)$ is non-zero for $\epsilon > X$. The modeling is most accurate for $kT_x < \epsilon < X$. Accuracy of the model for $\epsilon \simeq 0$ is difficult to determine without numerical solutions of greater resolution than are available. The limiting factor in such solutions is a combination of finite computer resources and lack of resolution in experimental cross-sections. The most accurate method of approximating $R(\epsilon)$ would seem to be to use some form of average R similar to

$$R = \frac{\int_{\epsilon_1}^{\epsilon_2} R(\epsilon')d\epsilon'}{\epsilon_2 - \epsilon_1} \qquad (3\text{-}7)$$

where ϵ_2 and ϵ_1 are the points where $R(\epsilon)$ is 0. However, in practice this method is not clearly adequate, for several reasons. For one thing, the analytic R extends an infinite distance up the energy axis; this makes it difficult to compare with a realistic rate that is of finite extent in energy space. Also, any such average, assuming one could be properly picked, would generally be tedious to evaluate, especially to produce what is at best an estimate. It appears that reasonably good results can be acheived by using R equal to one half the maximum value of $R(\epsilon)$ for the particular tran-

sition involved, and by choosing X equal to the energy loss of the transition.

The analytic three-level model can be used to model realistic three-level systems only if the cross-sections for the two excited levels overlap and the condition $X_1 < (X_2 - X_1)$ is met. The resulting solution can be used to predict pumping rates for the highest level within an order of magnitude or less. Good results can apparently be obtained by choosing R_1, R_2, X_1, and X_2 the same as in the two-level case.

Under some circumstances, the three-level system can be used to model multi-level systems. The thresholds must fall into two groups, such that, if X_1 is a representative threshold for the lower group, and X_2 a representative threshold for the higher, then $X_1 < (X_2 - X_1)$. There must be no intervals above the lowest threshold for which all the cross-sections are zero. Good results can apparently be obtained by letting the reaction rate for each group be the average of one half the maximum reaction rate for each level in the group, and by letting the threshold for each group be the average of the thresholds for each group. The pumping rate for the lowest transition in the higher group can apparently be estimated within an order of magnitude or less by an expression analogous to Eq (3-6).

It would be, in principle, quite straightforward to extend this solution to more levels, or to levels of arbitrary spacing, and such extensions would allow modeling of cases that cannot be modeled by the present case. However,

the algebra involved in such extension is quite involved.

It should be possible to extend the model to cases where $R(\epsilon)$ above threshold is zero by explicitly including such regions as separate areas for which a separate solution must be found. For example, if $R(\epsilon) = 0$ for $\epsilon_1 < \epsilon < \epsilon_2$, the Boltzmann equation could first be solved for $\epsilon > \epsilon_2$; that solution could be used to find $f(\epsilon)$ for $\epsilon_1 < \epsilon < \epsilon_2$, and so forth.

Bibliography

1. Brown, Sanborn C. Introduction to Electrical Discharges in Gases. New York, London, and Sydney: John Wiley and Sons, 1966.

2. Davydov, Alexandre Sergeyevitch. Quantum Mechanics. Ann Arbor, Michigan: NEO Press, 1966.

3. Elliott, C. J. and A. E. Greene. "Electron Energy Distributions in e-beam Generated Xe and Ar Plasmas," Journal of Applied Physics, 47(7): 2946-2553 (July 1976).

4. Engelhardt, A. G. and A. V. Phelps. "Elastic and Inelastic Collision Cross Sections in Hydrogen and Deuterium from Transport Coefficients," Physical Review, 131: 2115 (1963).

5. Frost, L. S. and A. V. Phelps. "Rotational Excitation and Momentum Transfer Cross-Sections for Electrons in H_2 and N_2 from Transport Coefficients," Physical Review, 127(5): 1621-1633 (September, 1962).

6. Kieffer, L. J. A Compilation of Electron Collision Cross Section Data for Modelling Gas Discharge Lasers (Joint Institute for Laboratory Astrophysics Information Center Report 13). Boulder, Colorado: Joint Institute for Laboratory Astrophysics Information Center, September 30, 1973.

7. Long, W. H., Jr., W. F. Bailey, and A. Garscadden. "Electron Drift Velocities in Molecular-Gas-Rare-Gas Mixtures," Physical Review A, 13(1): 471-475 (January 1976).

8. Lorrain, Paul and Dale R. Corson. Electromagnetic Fields and Waves (Second Edition). San Francisco: W. H. Freeman and Company, 1970.

9. Nielsen, Philip E., Deputy Department Head, Department of Physics, Air Force Institute of Technology, Wright-Patterson AFB. "On Numerical and Analytic Solutions of the Boltzmann Equation in Energy Space," (tentative title), unpublished paper.

10. ----- and G. H. Canavan. "Electron Cascade Theory in Laser-Induced Breakdown of Preionized Gases," Journal of Applied Physics, 44(9): 4224-25 (September 1973).

11. -----, -----, and S. D. Rockwood. "Breakdown of Deuterium with a Ruby Laser," Proceedings of the Institute of Electrical and Electronics Engineers, 59(4): 709-710 (April 1971).

12. Nighan, William L. "Electron Energy Distributions and collision Rates in Electrically Excited N_2, CO, and CO_2," Physical Review A, 2(5): 1989-2000 (November 1970).

13. Rockwood, Stephen D. "Elastic and Inelastic Cross Sections for Electron - Hg Scattering from Hg Transport Data," Physical Review A, 8(5): 2348-2358 (November 1973).

14. -----. "A Comparison of Laser Induced Gas Breakdown in Various Gases," Institute of Electrical and Electronics Engineers Journal of Quantum Electronics, 10(9): 732 (September 1974).

15. Seward, E. D., W. R. Ercoline, T. E. Gist, and H. L. Hastings. Technical Report on Program NGB. Air Force Institute of Technology, Wright-Patterson AFB, 1978.

Appendix A

Validity of Assumptions

$\frac{\epsilon}{kT} >> 1$.

This assumption may be validated by using the form for $T(\epsilon)$ developed in Chapter 2. It will be evaluated at $\epsilon = X$, since this is the worst case condition. From such an evaluation the following expression may be derived:

$$\dot{\epsilon} << 6n_o RX \tag{A-1}$$

For typical values of $n_o \sim 10^{19}$ /cm^3, $R \sim 10^{-10}$ cm^3/sec, and $X = 4$ eV (Ref 6), this gives

$$\dot{\epsilon} << 2.4 \times 10^{10} \text{ eV/sec} \tag{A-2}$$

This value may easily be compared with published results. From Brown, it is seen that

$$\dot{\epsilon} = \frac{e^2E^2\nu}{2m(\omega^2 + \nu^2)} \tag{A-3}$$

where

e is the electron charge
m is the electron mass
ν is the average collision frequency of the electrons with the background gas
ω is the frequency of the electric field
E is the amplitude of the electric field (Ref 1: 166)

For a DC field, $\omega = 0$. Also, since the average field strength is $\frac{\sqrt{2}}{2}$ times the amplitude of a sinusoidal field, but is equal to the amplitude of a DC field, $E^2/2$ becomes E^2. This leads to

$$\dot{\epsilon} = \frac{n_o{}^2 e^2 \left(\frac{E}{n_o}\right)^2}{m\nu} \qquad \text{(A-4)}$$

Using the same typical values as before, and $\nu = 10^{12}$ /sec (Ref 13: 2349) gives

$$\frac{E}{n_o} \ll 3.7 \times 10^{-16} \text{ V-cm}^2 \qquad \text{(A-5)}$$

This is just above typical lower values of E/n_o (Ref 12: 1992-1993). This result is a significant limitation on the range of complete validity of the analytic model. Note, however, that this assumption was used primarily to justify neglecting the contributions at some energy ϵ (above threshold) due to inelastic collisions at an energy $\epsilon > X$. If the assumption is no longer valid, then those contributions can no longer be neglected. Even so, the conclusion about the resolution required in numerical solutions are still valid.

For fields at optical frequencies, $\omega^2 + \nu^2 \simeq \omega^2$, and Eq (A-3) becomes

$$\dot{\epsilon} = \frac{e^2 E^2 \nu}{2m\omega^2} \qquad \text{(A-6)}$$

Recall that the average Poynting vector amplitude, S, is given by (Ref 8: 465)

$$S = \frac{c\epsilon_o E^2}{2} \tag{A-7}$$

Substituting Eq (A-7) and Eq (A-6) into Eq (A-1) results in

$$S << \frac{6n_o RX\omega^2 c\epsilon m}{e^2 \nu} \tag{A-8}$$

Using the same values as before and ω appropriate for a CO_2 laser results in

$$S << 1.2 \times 10^9 \text{ watts/cm}^2 \tag{A-9}$$

This is near or even above reported thresholds for breakdown in clear air (Refs 10; 11). It is certainly high enough to allow investigation of gas laser systems.

$\frac{1}{kT}\frac{\partial T}{\partial \epsilon} >> \frac{\partial^2 T}{\partial \epsilon^2}$

Evaluation of this expression for the $T(\epsilon)$ developed in Chapter II leads to a worst case of

$$\dot{\epsilon} << 24 n_o RX \tag{A-10}$$

This is obviously valid if Eq (A-1) is valid.

$n_x << n_o$

This assumption is used on several occasions to justify discarding terms $\sim n_x f(\epsilon)R(\epsilon)$. The worst case is for $\epsilon = 2X$. In this case the assumption is $n_x f(\epsilon - X) << n_o f(\epsilon)$. For $\epsilon > 2X$, this becomes

$n_x \exp\left[-\frac{\sqrt{X}\,\sqrt{(\epsilon - X)}}{kT_x}\right] \ll n_o \exp\left[\frac{-\sqrt{X\epsilon}}{kT_x}\right]$. This eventually becomes

$$\frac{n_o}{n_x} \gg \exp\left[\frac{(\sqrt{2} - 1)\,X}{kT_x}\right] \qquad \text{(A-11)}$$

Typical values of $\frac{X}{kT_x}$ range form 20 to 50; this gives values of $\exp(.414\,\frac{X}{kT_x})$ from $\sim 10^3$ to $\sim 10^9$. For atmospheric density of 3×10^{19} cm^3, this allows $n_o \ll 10^{10} - 10^{16}$. This is sufficient for a very large number of cases.

Importance of Elastic Collisions

It is very difficult at this time to precisely determine the effect of elastic collisions. Rockwood showed that elastic collisions could be ignored in mercury vapor for E/n_o greater than $\sim 2 \times 10^{-17}$ volts-cm (Ref 13: 2353). The elastic collision rate is proportional to the ratio of the electron mass to the background particle mass. Mercury is a very heavy particle, with a mass some 4.5 times heavier than CO_2, for instance. It would be expected that Rockwood's case would represent an extreme. Comparison of the heating term to the elastic collision term in the Boltzmann equation leads to the requirement that $X/kT_x \gtrsim 100$ for elastic collisions to be ignored, which is not inconsistent with the results above.

The best approach to this problem would be to repeat the derivation performed in this thesis, but with elastic collisions included. Unfortunately, that is beyond both the

scope and the time limitations of the present study.

Appendix B

Choice of q

General Considerations

Physical. Consider that $f(\epsilon)$, for $\epsilon < X$, depends on $f(\epsilon + X)$. The solution for $\epsilon \sim 0$ is affected most strongly by $f(\epsilon)$ for ϵ just above X (see Fig (B-1)). Since kT_x is characteristic of the energy range for which there is a significant change in $f(\epsilon)$, for $\epsilon > X$, it is not unreasonable to expect that the behavior of $f(\epsilon)$, for $\epsilon \sim 0$, might also change significantly over a range $\sim kT_x$.

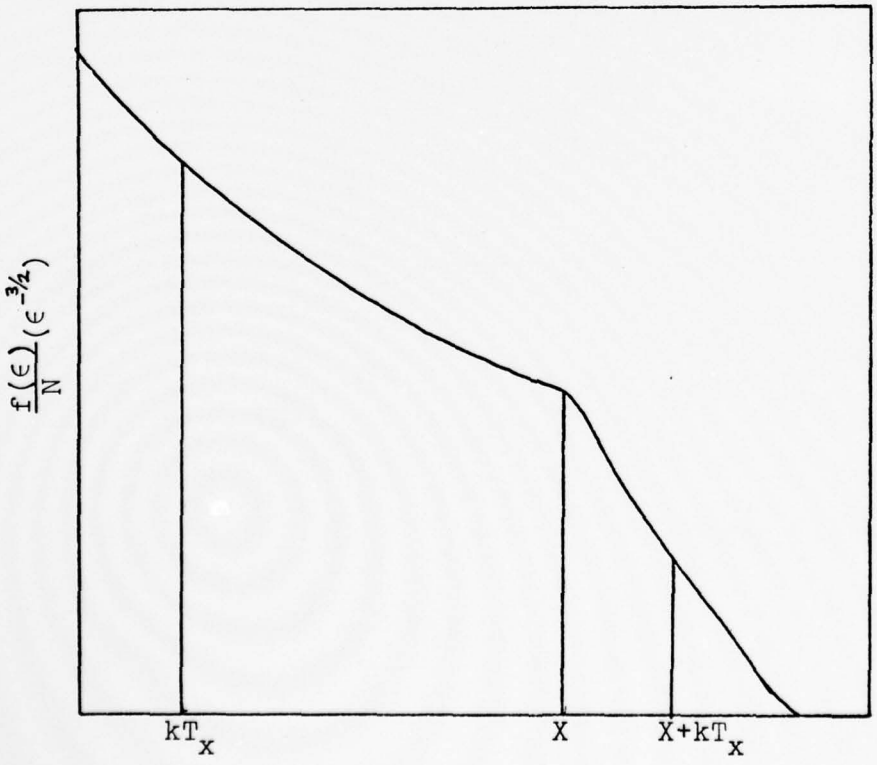

Figure B-1. Comparison of $f(\epsilon)$ $\epsilon \approx 0$ and $\epsilon \approx X$

Mathematical. There are several approaches that could be used to choose q. One would be to choose q so that N is insensitive to q; that is, choose q so that $dN(q)/dq = 0$. This has some physical significance in that q is strictly a result of the method used to solve the Boltzmann equation; its effect on the final solution should be as little as possible.

Another method would be to choose q so that $\partial f/\partial \epsilon$ is continuous at q. This approach is mathematically satisfying, but has little physical meaning, expecially when the equation for $\partial f/\partial \epsilon$ already had the discontinuous function $R(\epsilon)$. Regardless of the approach used, q must be chosen so that the approximations used in solving the equation for $\epsilon < X$ are valid.

Two-Level Model

$dN/dq = 0$. First the condition $dN/dq = 0$ was used to evaluate q. This led to a complex value for q, which was unacceptable. Since it was impossible to find a real value for q for which there was no dependence of N on q, an attempt was made to find a value of q which minimized the dependence of N on q by using the condition $d^2N/dq^2 = 0$. This led to $q = kT_x$.

Continuity of $df/d\epsilon$ at q. In order to use continuity of $df/d\epsilon$ to evaluate q, $df/d\epsilon$ was evaluated for $\epsilon < q$ and $\epsilon > q$, and the two expressions set equal. This led to a complex value for q, which is unacceptable. As a result,

the following procedure was used to choose q. Let $df(\epsilon)/d\epsilon_+ = df/d\epsilon$, for $\epsilon > q$, and $df(\epsilon)/d\epsilon_- = df/d\epsilon$, for $\epsilon < q$. Then let $\Delta(q) = df(q)/d\epsilon_+ - df(q)/d\epsilon_-$. Letting $d\Delta/dq = 0$ results in a value of q that minimizes the change in $df/d\epsilon$ at q. The value of q that resulted was $2kT_x$.

Validity of Assumptions. It is fairly easy to examine the validity of the assumptions involved in the solution for $\epsilon < q$. As was shown in Eq (2-15), for $\epsilon < q$, $\partial f/\partial \epsilon$ is given by

$$\frac{\partial f}{\partial \epsilon} = \frac{-c \exp[-X/kT_x]}{2kT_x} \frac{X^{3/2}}{\sqrt{\epsilon}} \sum_{n=1}^{\infty} \left(\frac{-\epsilon}{2kT_x}\right)^n \frac{1}{n!(n - \frac{1}{2})} \qquad \text{(B-1)}$$

where the validity of the solution is tested at $\epsilon = q$. The speed with which this converges is very sensitive to the choice of q. As an example, Table B-1 gives the values of A_n, where $A_n = \left(\frac{q}{2kT_x}\right)^n \frac{1}{n!(n - \frac{1}{2})}$, for $q = 2kT_x$, and $q = 3kT_x$.

n	A_n $q = kT_x$	A_n $q = 2kT_x$	A_n $q = 3kT_x$
1	1.0	2.0	3.0
2	.083	.3333	.75
3	.0083	.0667	.225
4	.00074	.0119	.06

Table B-1. Convergence of $\partial f/\partial \epsilon$

As can be seen, the choice of $q = kT_x$ allows retention of only the first two terms in the series with excellent results.

It is almost as simple to examine the assumption for $\epsilon \approx X$. By comparing the exact expression for the integral in equation (2-11) with approximate form actually used, it can be shown that the error is proportional to Δ, where Δ is given by

$$\Delta = \int_{\left(\frac{X}{kT_x}\right)\left(1 + \frac{\epsilon}{X}\right)^{\frac{1}{2}}}^{\sqrt{2}\left(\frac{X}{kT_x}\right)} u^2 e^{-u} du \qquad \text{(B-2)}$$

By evaluating both Δ and the similar expression in the approximate form, and utilizing the assumptions used throughout the derivation, it can be shown that the following condition is sufficient for the approximation to be valid:

$$1 >> \epsilon \exp\left(-\frac{X}{kT_x}\left(\sqrt{2} - \frac{\sqrt{2}}{4} - 1 + \sqrt{\frac{2}{4}}\,\frac{\epsilon}{X}\right)\right) \qquad \text{(B-3)}$$

This condition is much more sensitive to $\frac{X}{kT_x}$ than it is to $\frac{\epsilon}{X}$. For $\frac{X}{kT_x} = 30$, which is a typical value, Eq (C-3) leads to $1 >> .16$ for $\epsilon = 0$, and $1 >> .11$ for $\epsilon = kT_x$. This approximation is not as sound for $q = kT_x$ as is the approximation for $\epsilon << X$; however, increasing q would effect little improvement on the approximation for $\epsilon > kT_x$, and it would seriously degrade the approximation for $\epsilon < kT_x$.

Since the physical and mathematical arguments have already indicated that a choice of $q \approx kT_x$ is valid; and since it has just been shown that $q = kT_x$ results in valid results, that value was used.

Three-Level Model

Since the derivation for the three-level model is exactly analogous to the two-level derivation, the same choice of q would be valid, except that there are two different values for kT_x; kT_{x1} and kT_{x2}. Regardless of the choice of q, $f(\epsilon)$ should reduce to the two-level case for $X_1 = X_2$ and $R_2 = 0$. Under these circumstances, therefore, q should reduce to kT_x. In addition, note that $f(\epsilon)$ for $\epsilon < q$ is affected strongly by the behavior of $f(\epsilon)$ at $X_1 < \epsilon < X_1 + q$ and $X_2 < \epsilon < X_2 + q$ (see Fig (B-2)). Since $f(X_1) >> f(X_2)$, it is reasonable to expect that $f(\epsilon)$ at $\epsilon \approx 0$ is affected most strongly by $f(\epsilon)$ at $\epsilon \approx X_1$. For this reason the choice of $q = kT_{x1}$ was made.

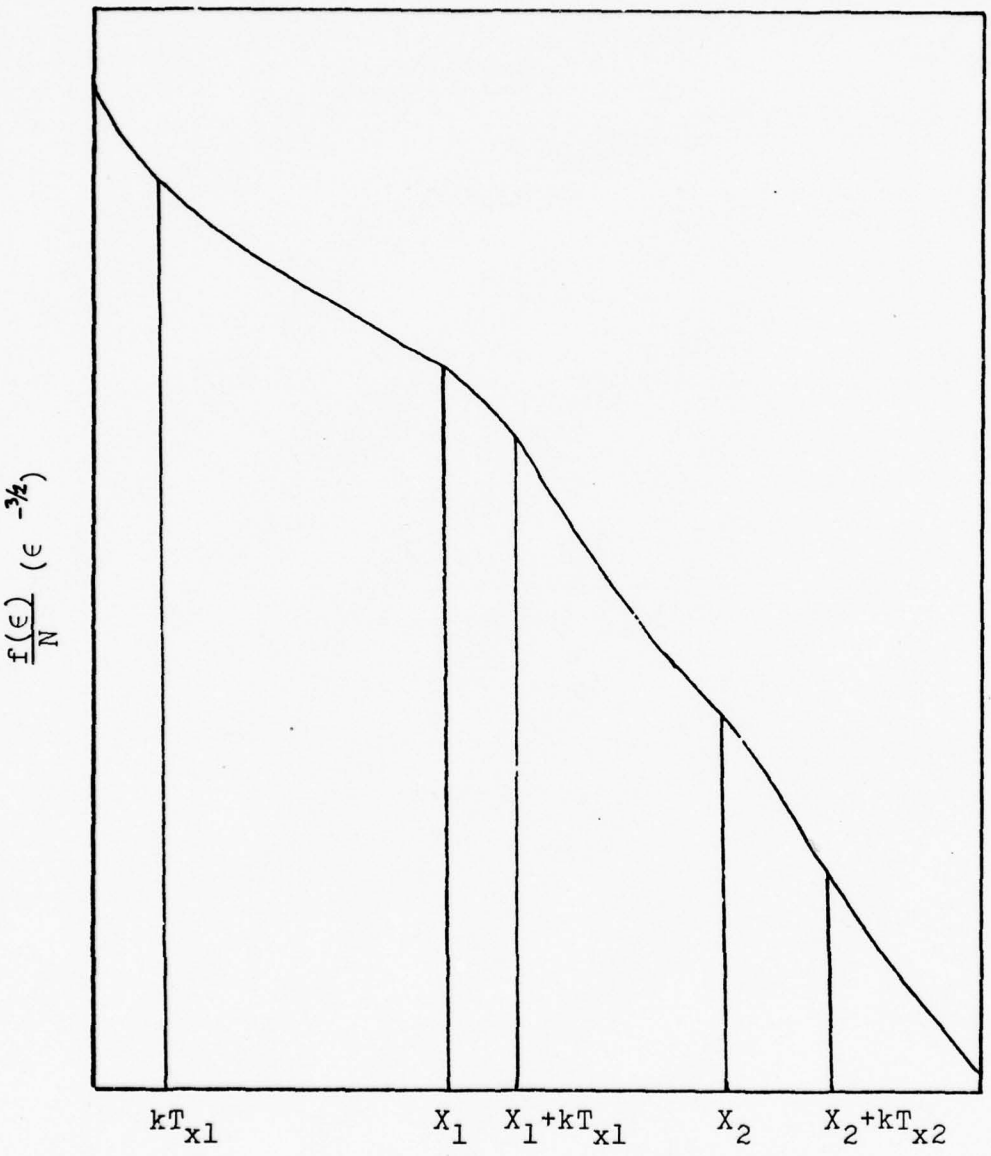

Figure B-2. Comparism of $f(\epsilon)$ for $\epsilon \quad X_1$ and $\epsilon \quad X_2$

Appendix C

NGB

General Description

NGB is a Fortran computer program that numerically solves the Boltzmann equation for conditions typical of electron-beam sustained discharge lasers. It can include effects due to field-driven ionization, electron-beam-driven ionization, excitation and de-excitation, heating by a constant electric field, electron-electron interactions, elastic collisions with the background species, and disassociative attachment due to reactions of the form $e + Cl_2 \longrightarrow Cl + Cl^-$. It integrates the Boltzmann equation to find a time-dependent $f(\epsilon)$. It continues to output $f(\epsilon)$ as a function of time until $f(\epsilon)$ is constant from one time step to the next. Note that since $f(\epsilon)$ represents the fraction of the total electron density at a particular energy, it is possible to reach a quasi-steady solution where $f(\epsilon)$ is constant, but n_e is increasing.

The integrator used in NGB is the IMSL-designed DVOGER. DVOGER is a variable-order Gear-type integrator; in NGB DVOGER will go as high as sixth order.

For a fuller explanation of NGB, see the AFIT Tech Report to be published in the fall of 1978, by Seward, Hastings, Ercoline, and Gist.

Particular Application

Program Modification. NGB was modified slightly for some portions of this thesis. The standard NGB calculates

the heating due to an externally applied field by calculating the average collision time for an electron of a particular energy with all the background species, and then calculating the current produced by those electrons under the influence of the external field. This produces an energy-dependent $\dot{\epsilon}$. Since the analytic model assumed a constant $\dot{\epsilon}$, NGB was modified to return a constant $\dot{\epsilon} = 2 \times 10^{8}$ eV/sec for all solutions.

Input Parameters. NGB allows the user to select which effects he wishes to include. For this thesis the input program switches were set to include only the effects of heating (subroutine HEAT) and non-ionizing inelastic and superelastic collisions (subroutine XCITE). An initial and minimum timestep of 1×10^{-14} seconds was used. The internal error parameter for DVOGER was set at .001. The maximum allowed convergence difference, which defines the convergence condition, was set to 1×10^{-10}.

Appendix D

TI-59 Programs

General

The following programs allow calculation of the values of the analytic two or three level solutions on a Texas Instrument Programmable 59 calculator. The program for the two-level solution requires 177 steps; the program for the three-level requires 477 steps. Each program is segmented, and could be run a segment at a time on a TI-58 calculator; however, since the TI-58 does not allow automatic program readin, this would be a time consuming procedure.

Two-Level Program

Program Listing. Table D-1 gives the program listing for the two-level program.

Step	Key Code	Operation	Comment
000	76	LBL	
	11	A	
	43	RCL	
	00	00	Find
	55	÷	$\frac{X}{kT_x}$
	43	RCL	
	01	01	
	95	=	
	42	STO	
	04	04	
010	45	y^x	
	03	3	Find N
	95	=	
	35	1/X	

Step	Key Code	Operation	Comment
014	65	x	
	04	4	
	85	+	
	43	RCL	
	04	04	
	33	X^2	
020	35	1/X	
	65	x	
	04	4	
	85	+	
	43	RCL	
	04	04	
	35	1/X	
	65	x	
	02	2	
	85	+	
030	43	RCL	
	04	04	
	55	÷	
	03	3	
	85	+	
	07	7	
	55	÷	
	01	1	
	08	8	
	95	=	
040	65	x	
	53	(	
	43	RCL	
	00	00	
	34	$\sqrt{X}$	
	45	y^x	
	03	3	
	54	)	
	95	=	

Step	Key Code	Operation	Comment
049	42	STO	
050	05	05	
	43	RCL	
	04	04	Find Constant
	34	$\sqrt{X}$	term in
	65	x	Eq (2-18)
	01	1	for $\epsilon < kT_x$
	07	7	
	55	÷	
	01	1	
	02	2	
060	75	-	
	01	1	
	95	=	
	65	x	
	43	RCL	
	04	04	
	85	+	
	01	1	
	95	=	
	42	STO	
070	06	06	
	43	RCL	
	05	05	Display N
	91	R/S	
	76	LBL	
	12	B	
	43	RCL	
	02	02	Increment ϵ
	44	SUM	and display
	03	03	
080	43	RCL	
	03	03	
	66	PAUSE	
	34	$\sqrt{X}$	
	45	y^x	

Step	Key Code	Operation	Comment
085	03	3	Calculate
	95	=	$f(\epsilon)/n$, for
	55	÷	$\epsilon < kT_x$
	03	3	
	55	÷	
090	43	RCL	
	01	01	
	75	-	
	02	2	
	65	x	
	43	RCL	
	03	03	
	34	$\sqrt{X}$	
	95	=	
	65	x	
100	43	RCL	
	00	00	
	34	$\sqrt{X}$	
	45	y^x	
	03	3	
	55	÷	
	04	4	
	55	÷	
	43	RCL	
	01	01	
110	33	X^2	
	85	+	
	43	RCL	
	06	06	
	95	=	
	55	÷	
	43	RCL	
	05	05	
	95	=	
	91	R/S	

Step	Key Code	Operation	Comment
120	76	LBL	
	13	C	
	43	RCL	
	02	02	Increment ϵ
	44	SUM	
	03	03	
	43	RCL	
	00	00	
	55	÷	
	43	RCL	
130	03	03	Display ϵ
	66	PAUSE	
	95	=	
	34	$\sqrt{X}$	Calculate
	75	-	$f(\epsilon)/N$, for
	01	1	$kT_x < \epsilon < X$
	95	=	
	65	x	
	43	RCL	
	04	04	
140	85	+	
	01	1	
	95	=	
	55	÷	
	43	RCL	
	05	05	
	95	=	
	91	R/S	
	76	LBL	
	14	D	
150	43	RCL	
	02	02	Increment ϵ
	44	Sum	and display
	03	03	
	43	RCL	
	03	03	

Step	Key Code	Operation	Comment
156	66	PAUSE	
	55	÷	
	43	RCL	Calculate
	00	00	f(∈)/N, for
160	95	=	∈ < X
	34	$\sqrt{X}$	
	94	+/-	
	85	+	
	01	1	
	95	=	
	65	x	
	43	RCL	
	04	04	
	95	=	
170	22	INV	
	23	LNX	
	55	÷	
	43	RCL	
	05	05	
	95	=	
176	91	R/S	

Table D-1. Program for Two-Level Model

Program Use. First, X is stored in register 00, kT_x in register 01, d∈ in register 02, and an initial value of ∈ in 03. Pressing key A causes the calculator to evaluate N, storing it in register 05, and to evaluate the constant expressions $1 + \frac{X}{kT_x}\left[\frac{17}{12}\left(\frac{X}{kT_x}\right)^{\frac{1}{2}} - 1\right]$ in equation (2-18) and store it in register 06. Pressing key B causes the calculator to increment ∈ by d∈, display the new ∈ momentarily, and then calculate and display f(∈), using the expression valid

for $\epsilon < kT_x$. Pressing key C similarly calculates $f(\epsilon)$ for $kT_x < \epsilon < X$; D calculates $f(\epsilon)$ for $X < \epsilon$. Note that the program does not check to insure that the value of ϵ and the form of $f(\epsilon)$ are compatible.

Three-Level Program

Program Listing. Table D-2 gives the program listing for the three-level program.

Step	Key Code	Operation	Comment
000	76	LBL	
	45	y^x	Subroutine
	53	(	that
	34	$\sqrt{X}$	calculates
	45	y^x	X
	03	3	
	54	)	
	92	INV SBR	
	76	LBL	
	12	B	
010	43	RCL	
	03	03	Increment ϵ
	44	SUM	and display
	04	04	
	43	RCL	
	04	04	
	66	PAUSE	
	34	$\sqrt{X}$	
	35	1/X	Calculate
	75	-	$f(\epsilon)/N$ for
020	43	RCL	$kT_{x1} < \epsilon < X_1$
	01	01	
	34	$\sqrt{X}$	
	35	1/X	
	54	)	

Step	Key Code	Operation	Comment
025	55	÷	
	02	2	
	65	x	
	43	RCL	
	07	07	
030	85	+	
	43	RCL	
	30	30	
	54	)	
	55	÷	
	43	RCL	
	09	09	
	54	)	
	91	R/S	
	76	LBL	
040	13	C	
	43	RCL	
	03	03	Increment ϵ
	44	SUM	and display
	04	04	
	43	RCL	
	04	04	
	66	PAUSE	
	55	÷	
	43	RCL	Calculate
050	02	02	$f(\epsilon)/N$,
	54	)	$X_1 < \epsilon < X_2$
	34	$\sqrt{X}$	
	94	+/-	
	85	+	
	01	1	
	54	)	
	65	x	
	43	RCL	
	01	01	
060	34	$\sqrt{X}$	

Step	Key Code	Operation	Comment
061	65	x	
	43	RCL	
	02	02	
	34	$\sqrt{X}$	
	55	÷	
	43	RCL	
	11	11	
	54	)	
	22	INV	
070	23	LNX	
	55	÷	
	43	RCL	
	09	09	
	54	)	
	91	R/S	
	76	LBL	
	14	D	
	43	RCL	
	03	03	Increment ϵ
080	44	SUM	and display
	04	04	
	43	RCL	
	04	04	
	66	PAUSE	
	55	÷	
	43	RCL	Calculate
	02	02	$f(\epsilon)/N$, for
	54	)	$X_2 < \epsilon$
	34	$\sqrt{x}$	
090	94	+/-	
	85	+	
	01	1	
	54	)	
	65	x	
	43	RCL	
	02	02	

Step	Key Code	Operation	Comment
097	55	÷	
	43	RCL	
	21	21	
100	54	)	
	22	INV	
	23	LNX	
	55	÷	
	43	RCL	
	09	09	
	54	)	
	91	R/S	
	76	LBL	
	11	A	
110	43	RCL	
	03	03	Increment ϵ
	44	SUM	and display
	04	04	
	43	RCL	
	04	04	
	66	PAUSE	
	71	SBR	
	45	y^x	Calculate $f(\epsilon)$
	55	÷	$\epsilon < kT_{x1}$
120	02	2	
	04	4	
	55	÷	
	43	RCL	
	11	11	
	75	-	
	43	RCL	
	04	04	
	34	$\sqrt{x}$	
	55	÷	
130	04	4	
	54	)	
	65	x	

Step	Key Code	Operation	Comment
133	43	RCL	
	01	01	
	71	SBR	
	45	y^x	
	55	÷	
	43	RCL	
	12	12	
140	65	x	
	43	RCL	
	30	30	
	85	+	
	53	(	
	43	RCL	
	04	04	
	71	SBR	
	45	y^x	
	55	÷	
150	02	2	
	04	4	
	55	÷	
	43	RCL	
	21	21	
	75	-	
	43	RCL	
	04	04	
	34	$\sqrt{x}$	
	55	÷	
160	04	4	
	54	)	
	65	x	
	43	RCL	
	40	40	
	65	x	
	43	RCL	
	02	02	

Step	Key Code	Operation	Comment
168	71	SBR	
	45	y^x	
170	55	÷	
	43	RCL	
	22	22	
	85	+	
	43	RCL	
	08	08	
	54	)	
	55	÷	
	43	RCL	
	09	09	
180	54	)	
	91	R/S	
	76	LBL	
	16	A'	
	43	RCL	
	11	11	Calculate and store $(kT_{x1})^2$
	33	X^2	
	42	STO	
	12	12	
	65	x	
190	43	RCL	Calculate and store $(kT_{x1})^3$
	11	11	
	54	)	
	42	STO	
	13	13	
	43	RCL	
	21	21	Calculate and store $(kT_{x2})^2$
	33	X^2	
	42	STO	
	22	22	
200	65	x	
	43	RCL	Calculate and store
	21	21	

Step	Key Code	Operation	Comment
203	54	)	$(kT_{x2})^3$
	42	STO	
	23	23	
	02	2	
	65	x	Calculate N;
	53	(	store in R 09
	43	RCL	(here until
210	02	02	step 364)
	34	$\sqrt{X}$	
	65	x	
	43	RCL	
	21	21	
	85	+	
	02	2	
	65	x	
	43	RCL	
	22	22	
220	55	÷	
	43	RCL	
	02	02	
	34	$\sqrt{X}$	
	85	+	
	02	2	
	65	x	
	43	RCL	
	23	23	
	55	÷	
230	43	RCL	
	02	02	
	71	SBR	
	45	y^x	
	75	-	
	43	RCL	
	02	02	
	65	x	

Step	Key Code	Operation	Comment
238	43	RCL	
	11	11	
240	55	÷	
	43	RCL	
	01	01	
	34	$\sqrt{X}$	
	75	-	
	02	2	
	65	x	
	43	RCL	
	12	12	
	65	x	
250	43	RCL	
	02	02	
	34	$\sqrt{X}$	
	55	÷	
	43	RCL	
	01	01	
	75	-	
	02	2	
	65	x	
	43	RCL	
260	13	13	
	55	÷	
	43	RCL	
	01	01	
	71	SBR	
	45	y^x	
	54	)	
	85	+	
	43	RCL	
	30	30	
270	65	x	
	53	(	
	02	2	
	65	x	

Step	Key Code	Operation	Comment
274	43	RCL	
	01	01	
	34	$\sqrt{X}$	
	65	x	
	43	RCL	
	11	11	
280	85	+	
	04	4	
	65	x	
	43	RCL	
	12	12	
	55	÷	
	43	RCL	
	12	12	
	55	÷	
	43	RCL	
	01	01	
	34	$\sqrt{X}$	
	85	+	
290	04	4	
	65	x	
	43	RCL	
	13	13	
	55	÷	
	43	RCL	
	01	01	
	71	SBR	
	45	y^x	
	85	+	
300	43	RCL	
	01	01	
	71	SBR	
	45	y^x	
	65	x	
	43	RCL	
	01	01	

Step	Key Code	Operation	Comment
307	55	÷	
	06	6	
	55	÷	
310	43	RCL	
	11	11	
	85	+	
	01	1	
	09	9	
	65	x	
	43	RCL	
	01	01	
	71	SBR	
	45	y^x	
320	55	÷	
	03	3	
	06	6	
	54	)	
	85	+	
	43	RCL	
	40	40	
	55	÷	
	06	6	
	65	x	
330	43	RCL	
	02	02	
	71	SBR	
	45	y^x	
	55	÷	
	43	RCL	
	21	21	
	65	x	
	53	(	
	43	RCL	
340	01	01	
	75	-	

Step	Key Code	Operation	Comment
342	43	RCL	
	11	11	
	75	-	
	43	RCL	
	13	13	
	55	÷	
	01	1	
	02	2	
350	55	÷	
	43	RCL	
	22	22	
	85	+	
	43	RCL	
	12	12	
	55	÷	
	04	4	
	55	÷	
	43	RCL	
360	21	21	
	54	)	
	54	)	
	42	STO	
	09	09	
	43	RCL	
	30	30	Calculate
	65	x	constant term
	53	(	in Eq (2-21)
	01	1	for $\epsilon < kT_{x1}$;
370	07	7	store in R 08
	55	÷	(here until
	02	2	step 449)
	04	4	
	65	x	
	53	(	
	43	RCL	
	01	01	

Step	Key Code	Operation	Comment
378	55	÷	
	43	RCL	
380	11	11	
	54	)	
	71	SBR	
	45	y^x	
	75	-	
	43	RCL	
	01	01	
	55	÷	
	02	2	
	55	÷	
390	43	RCL	
	11	11	
	85	+	
	01	1	
	54	)	
	85	+	
	43	RCL	
	40	40	
	55	÷	
	02	2	
400	65	x	
	43	RCL	
	02	02	
	71	SBR	
	45	y^x	
	65	x	
	53	(	
	43	RCL	
	11	11	
	34	$\sqrt{x}$	
410	55	÷	
	02	2	
	55	÷	
	43	RCL	

Step	Key Code	Operation	Comment
414	22	22	
	75	-	
	43	RCL	
	11	11	
	71	SBR	
	45	y^x	
420	55	÷	
	01	1	
	02	2	
	55	÷	
	43	RCL	
	23	23	
	85	+	
	53	(	
	43	RCL	
	21	21	
430	65	x	
	43	RCL	
	11	11	
	34	$\sqrt{X}$	
	54	)	
	35	1/X	
	75	-	
	53	(	
	43	RCL	
	21	21	
440	65	x	
	43	RCL	
	01	01	
	34	$\sqrt{X}$	
	54	)	
	35	1/X	
	54	)	
	54	)	
	42	STO	

Step	Key Code	Operation	Comment
449	08	08	
450	43	RCL	
	30	30	Calculate
	65	x	constant factor
	43	RCL	in Eq (2-21),
	01	01	for
	71	SBR	$kT_{x1} < \epsilon < kT_{x2}$
	45	y^x	store in R 07
	55	÷	
	43	RCL	
	11	11	
460	85	+	
	43	RCL	
	40	40	
	65	x	
	43	RCL	
	02	02	
	71	SBR	
	45	y^x	
	55	÷	
	43	RCL	
470	21	21	
	54	)	
	42	STO	
	07	07	
	43	RCL	
	09	09	Display N
476	91	R/S	

Table D-2. Program for Three-Level Model

Program Use. First, initial parameters are loaded as in Table D-3.

AD-A064 213 AIR FORCE INST OF TECH WRIGHT-PATTERSON AFB OHIO SCH--ETC F/G 20/5
ANALYTIC ELECTRON ENERGY DISTRIBUTION FUNCTIONS FOR ELECTRIC DI--ETC(U)
DEC 78 T E GIST

UNCLASSIFIED AFIT/GEP/PH/78D-4 NL

2 OF 2
AD A064213

END
DATE FILMED
4-79
DDC

Register	Content
01	X_1
02	X_2
03	$d\epsilon$
04	ϵ (usually 0 initially)
11	kT_{x1}
21	kT_{x2}
30	$\exp\left[\frac{\sqrt{X_1X_2} - X_1}{kT_{x1}}\right]$
40	$\frac{R_1}{R_1 + R_2}$

Table D-3. Initial Parameters

Then key A' is pressed. The calculator evaluates additional parameters, stores them as shown in Table D-4, and displays N.

Register	Contents
07	$\exp\left[\frac{\sqrt{X_1X_2} - X_1}{kT_{x1}}\right] \frac{X_1^{3/2}}{kT_{x1}} + \frac{R_1}{R_1 + R_2} \frac{X_2^{3/2}}{kT_{x2}}$
08	Constant term in Equation (2-23), $\epsilon < kT_{x1}$. Term starts "$\exp\left[\frac{\sqrt{X_1X_2} - X_1}{kT_{x1}}\right]\left(\frac{17}{24} \ldots\ldots$ and ends $\cdots - \frac{1}{kT_{x2}(X_1)}\right\}$"
09	N
12	$(kT_{x1})^2$
13	$(kT_{x1})^3$

Register	Contents
22	$(kT_{x2})^2$
23	$(kT_{x2})^3$

Table D-4. Post-Initialization Parameters

From this point, pressing A, B, C, or D causes the calculator to increment ϵ by $d\epsilon$. and calculate $f(\epsilon)$, using the expression for $\epsilon < kT_{x1}$, $kT_{x1} < \epsilon < X_1$, $X_1 < \epsilon < X_2$, or $X_2 < \epsilon$, respectively, depending on which key is pressed. Again, the program does not test to see that ϵ and the expression for $f(\epsilon)$ are compatible.

VITA

Thomas E. Gist was born on 12 December 1949 in Dallas, Texas. He graduated from high school in Fort Worth, Texas in 1968 and received the degree of Bachelor of Science from Texas Christian University in May, 1972. Upon receiving his Air Force commission through ROTC, he entered active duty in July, 1972, as a Space Surveillance Officer at Detachment 7, 14th Missile Warning Squadron, MacDill AFB, Florida. After serving as the Operations Officer, Det 2, 18th Surveillance Squadron, Johnston Island AFB, Johnston Atoll, and as a Missile Warning Monitor, Missile Warning Officer, Launch Correlation Unit Duty Officer, Chief, Launch Correlation Unit, and Assistant Chief, Missile Warning Operations Division, at the NORAD Combat Operations Center, NORAD Cheyenne Mountain Complex, Colorado, he entered the School of Engineering, Air Force Institute of Technology, in June 1977.

Permanent address: 5300 Odessa Ave
Fort Worth, Texas 76133

UNCLASSIFIED

SECURITY CLASSIFICATION OF THIS PAGE *(When Data Entered)*

REPORT DOCUMENTATION PAGE		READ INSTRUCTIONS BEFORE COMPLETING FORM
1. REPORT NUMBER AFIT/GEP/PH/78D-4	2. GOVT ACCESSION NO.	3. RECIPIENT'S CATALOG NUMBER
4. TITLE *(and Subtitle)* ANALYTIC ELECTRON ENERGY DISTRIBUTION FUNCTIONS FOR ELECTRIC DISCHARGE LASERS		5. TYPE OF REPORT & PERIOD COVERED MS Thesis 6. PERFORMING ORG. REPORT NUMBER
7. AUTHOR(s) Thomas E. Gist Capt		8. CONTRACT OR GRANT NUMBER(s)
9. PERFORMING ORGANIZATION NAME AND ADDRESS AF Inst of Tech (AFIT-EN) Wright-Patterson AFB Ohio 45433		10. PROGRAM ELEMENT, PROJECT, TASK AREA & WORK UNIT NUMBERS
11. CONTROLLING OFFICE NAME AND ADDRESS Electric Lasers Branch (AFWL-ALE) Air Force Weapons Laboratory Kirtland AFB NM		12. REPORT DATE December 1978 13. NUMBER OF PAGES 99
14. MONITORING AGENCY NAME & ADDRESS *(if different from Controlling Office)*		15. SECURITY CLASS. *(of this report)* Unclassified 15a. DECLASSIFICATION/DOWNGRADING SCHEDULE

16. DISTRIBUTION STATEMENT *(of this Report)*

Approved for public release; distribution unlimited.

17. DISTRIBUTION STATEMENT *(of the abstract entered in Block 20, if different from Report)*

18. SUPPLEMENTARY NOTES

Approved for Public Release; IAW AFR 190-17.

J. P. HIPPS, Major, USAF
Director of Information 1-23-79

19. KEY WORDS *(Continue on reverse side if necessary and identify by block number)*

Electric Discharge Laser
Laser
Electric Discharge
Electron Distribution function
Laser-induced breakdown

20. ABSTRACT *(Continue on reverse side if necessary and identify by block number)*

The Boltzmann equation for electrons is solved for background gases of one or two excited levels under conditions typical of electric discharge lasers. Reaction rates are assumed constant above a threshold energy, and the electron heating rate is assumed independent of energy. Elastic and superelastic collisions were not considered. Numerical solutions from a program developed in conjunction with Seward, Hastings, and Ercoline are in excellent agreement with the analytic solutions.

DD FORM 1 JAN 73 1473 EDITION OF 1 NOV 65 IS OBSOLETE

UNCLASSIFIED

SECURITY CLASSIFICATION OF THIS PAGE *(When Data Entered)*

The analytic solutions are compared to numerical solutions that use realistic cross-sections; the analytic solutions agree well for some cross-sections. It is possible to determine a priori which realistic cases the analytic model will fit. For these cases it is possible to estimate pumping rates for upper levels with reasonable success. In some cases it is possible to model systems with more than two excited levels. Limitations to the analytic model and validity of the assumptions are discussed. Programs for evaluating the analytic solutions on a Texas Instruments Programmable 59 calculator are included.